Thesis

AI driven segmentation of abdominal fat compartments

submitted by

Robert Piber

in partial fulfillment of the requirements for the degree of

Doktor der gesamten Heilkunde
(Dr. med. univ.)

at the

Medical University of Graz

executed at the
Department of Radiology

under the supervision of
Gernot Reishofer, PhD
Eva Hassler, MD

Graz, 13.11.2022

Declaration of Academic Integrity

I hereby confirm that the present diploma thesis is the result of my own independent scholarly work. I also confirm that in all cases, where material from the work of others (in books, articles, essays, dissertations, and on the internet) is acknowledged, quotations and paraphrases are clearly indicated. No material other than that cited in the reference list has been used. I have read and understood the Medical University's regulations and procedures concerning plagiarism.

Graz, 16.10.2022 *Robert Piber m.p.*

Table of contents

Abbreviations

AAT = abdominal adipose tissue (= VAT + SAT)

AI = artificial intelligence

AT = adipose tissue

BMI = body mass index

CVD = cardiovascular disease

FSN = FatSegNet

HDL = high-density lipoprotein

IMAT = intermuscular adipose tissue (definition and differentiation: see chapter 1.1.4)

L1 = first lumbar vertebra

L5 = fifth lumbar vertebra

LDL = low density lipoprotein

MetS = metabolic syndrome

MRI = magnetic resonance imaging

QOL = quality of life

SAT = subcutaneous adipose tissue

TAG = triacylglyceride

TG = triglyceride

US = ultrasound (B-mode)

VAT = visceral adipose tissue

WHO = World Health Organisation

List of figures

List of tables

Zusammenfassung

Der Einsatz von künstlicher Intelligenz (KI) in der Radiologie wird immer wichtiger, um die Analyse und Interpretation der wachsenden Datenmengen zu beschleunigen, die durch die sich ständig verbessernde und weiter verbreitete Bildgebungstechnologie generiert werden. KI kann in Bereichen wie diesem erfolgreich eingesetzt werden, wo es schwierig ist, eine Korrelation zwischen eingehenden und ausgehenden Daten mathematisch zu formulieren.

Angesichts einer bereits hohen und ständig wachsenden Zahl von übergewichtigen und fettleibigen Menschen und damit zusammenhängenden Erkrankungen werden effizientere und genauere Methoden zur Messung der Körperzusammensetzung – möglicherweise KI-gesteuert – benötigt.

115 junge, mehrheitlich gut trainierte Proband*innen wurden mit der Dixon-MRT-Technik untersucht und die Daten wurden anschließend in zwei vollautomatische Segmentierungsalgorithmen eingespeist – einer davon deep-learning-basiert (*FatSegNet*), der andere nicht (ein k-Means-basierter Clustering-Algorithmus), um das Volumen des Fettgewebes (= adipose tissue = AT) innerhalb der Kompartimente zu bestimmen. Darüber hinaus wurden dieselben Proband*innen per Ultraschall (US) untersucht. Die mit den unterschiedlichen Methoden generierten Ergebnisse wurden dann miteinander verglichen und auf geschlechtsspezifische Unterschiede hinsichtlich der Verteilung von AT über das viszerale (VAT) und subkutane (SAT) Kompartiment untersucht.

Die abschließende Analyse wurde an 92 Proband*innen (48 Frauen, 44 Männer, 23.53 +/- 2.84 Jahre alt) durchgeführt. Die von beiden Algorithmen gemessenen Werte für die Volumina der AT-Kompartimente korrelieren gut, und die US-Messung des SAT korreliert eng mit den von beiden Algorithmen gemessenen SAT-Volumina.

Insgesamt stimmen die im Rahmen dieser Arbeit gewonnenen Daten mit der aktuellen Literatur überein, indem sie zeigen, dass die automatische Segmentierung von AT sehr genau ist - umso mehr, wenn sie von einem Deep-Learning-basierten Algorithmus durchgeführt wird. Auch die US-basierte Messung des SAT ist sehr genau und zuverlässig, insbesondere wenn sie von erfahrenen Untersucher*innen durchgeführt wird, die eine hoch entwickelte und standardisierte Methode anwenden. Schließlich stimmen unsere Daten mit dem aktuellen Verständnis des sexuellen Dimorphismus in AT-Verteilungsmustern überein, wobei Frauen relativ mehr gesamtes AAT (= abdominal AT = SAT+VAT) und SAT, und Männer relativ mehr VAT haben.

Abstract

The use of artificial intelligence (AI) in radiology becomes ever more important as a way to speed up analysis and interpretation of the growing amounts of data generated by constantly improving and more widely used imaging technology. AI can be applied successfully in areas like this one, where mathematically formulating a correlation between ingoing and outgoing data proofs difficult.

In the light of an already high and ever-growing number of overweight and obese people and obesity-related disorders, more efficient and accurate methods for measuring body composition – potentially AI driven - are needed.

115 young, mostly well-trained subjects were examined via the Dixon MRI technique and the data was subsequently fed into two fully automatic segmentation algorithms – one is deep-learning-based (*FatSegNet)*, the other one is not (a k-means-based clustering algorithm), in order to learn the volume of the adipose tissue (AT) within the compartments. Furthermore, the same subjects were examined via ultrasound (US). The results generated by the different methods were then compared to each other and examined for sex differences concerning the distribution of AT over the visceral (VAT) and subcutaneous (SAT) compartments.

The final analysis was performed on 92 subjects (48 females, 44 males, aged 23.53 +/- 2.84 years). The values for the volumes of the AT compartments measured by both algorithms correlate well, and the US measurement of SAT correlates tightly with the SAT volumes measured by both algorithms.

Overall, the data acquired via this thesis is congruent with the current literature in showing that automatic segmentation of AT is highly accurate, even more so when done by a deep-learning-based algorithm. Also, US-based measurement of (SAT) is highly accurate and reliable, especially if done by experienced examiners implementing a sophisticated and highly standardized method. Lastly, our data is in line with the current understanding of sexual dimorphism in AT distribution patterns, with females having relatively more overall AAT (= abdominal AT = SAT+VAT) and more SAT, and males having relatively more VAT.

1 Introduction

This thesis, “AI driven segmentation of abdominal fat compartments”, deals with different segmentation methods for assessing the amount and distribution of abdominal adipose tissue (AAT) in magnetic resonance imaging (MRI) data and its relationship to ultrasound (US) measurements of subcutaneous adipose tissue (SAT), and to other anthropometric measurements like body mass index (BMI). The aim is to compare the results each method provides and to highlight differences between females and males. An exact quantification especially of visceral and abdominal adipose tissue is essential, and MRI is the most reliable method for quantifying visceral adipose tissue (VAT) that is also not dependent on the use of ionizing radiation. The amount of VAT in particular is associated with metabolic dysfunction and its impact on chronic disease, quality of life, life span, and health span.

1.1 How too much fat can lead to disease

Over the course of the last four to five decades, a public health crisis established itself in the form of an ever-growing number of overweight and obese people and the illnesses connected to that. The global rate of obesity has nearly tripled since 1975 [1], while the number of global deaths attributed to obesity nearly doubled since 1990, with the number of people dying prematurely from obesity each year sitting at about 4.7 million. Roughly 8 % of global deaths are attributable to obesity. The numbers vary strongly between regions of the world. In typical western nations the number is closer to 10 %, whereas in low-income countries like in sub-Saharan Africa it is below 5 %. Also, the rate of obesity itself is highly diverse around the globe, and strongly correlated to a regions socioeconomic status, and to the alignment of its nutritional habits to typically western ones. The USA and middle eastern countries like Saudi Arabia are leading the charts, with rates of 36.2 % and 35.4 %, respectively. In the USA, 6 % of the population are morbidly obese, even (BMI > 40 kg/m²) [2]. The lowest rates are presented by Vietnam with 2.1 %, and India and Cambodia with 3.9 %. The European countries find themselves mostly with rates between 20 and 25 %, with Austria among them at 20.1 % [3].

Children are not spared either: In children, being overweight is defined by the child being two standard deviations above the median weight for their height, according to the WHO child growth standards [1]. By this definition, the number of overweight children has more than quadrupled since 1975.

Also, the financial cost of high BMI is significant: It is estimated by the WHO to amount to 990 billion US Dollars per year in expenditures for health-care services. The costs are direct (in- and outpatient treatments) and indirect (e.g. value of lost work, insurance) [4].

These alarming statistics make it all the more important to bring to even wider public recognition that the metabolic syndrome or a dysfunctional energy and fat metabolism in general are central driving forces in many of the most pressing health issues in the developed world [5].

1.1.1 Energy and fat metabolism

Like every system in the human body, the energy metabolism also needs to be in balance, or in homeostasis. This entails, that over a given period the amount of energy introduced into the system roughly equals the amount of energy expended. As long as this is the case, the bodyweight is maintained, even though changes in body composition are possible (e.g., loss of a certain amount of adipose tissue and simultaneous gain of a similar amount of muscle tissue [6], or the other way around). Also, changes in bodyweight having little to do with energy metabolism are possible, e.g., loss of stored glycogen and water weight when beginning a ketogenic maintenance diet, loss of water weight through the means of sweating or certain drugs (e.g., diuretics) or weight gain through foods that cause bloating or water retention, etc., though these factors will not be taken into consideration with this thesis. [7], [8], [9]

So, in general energy metabolism is about changing energy from one form (e.g., glucose, fatty acids) into another (e.g., mechanical energy for movement; energy to run diverse cellular processes; heat). Depending on the circumstances, the metabolism can work in an anabolic way, which means that supplied energy is used to build complex, organic macromolecules (fats, proteins, carbohydrates). If these

same macromolecules are split up for (mechanical) work or heat production, the metabolism is working in a catabolic way. [7], [8]

Energy is introduced into the system via food intake and use of the body's energy stores, the two most important of which are intramuscular as well as hepatic glycogen stores and white adipose tissue (AT), which has a cellular structure built on a single, large lipid droplet (making the cell turn "white" (=empty) after the fat droplet is emptied during histological preparation), which squeezes the other cellular content towards the periphery of the cell. Also, amino acids can be used for energy, though they make up only around 5 % of the basal metabolic rate (BMR). Therefore, their use for energy will be minimized, except when the body's carbohydrate stores run low, e.g., during fasting, where up to 15 % of the BMR can be provided by amino acids. [7], [8], [10]

Energy is used up by all cells in the body for processes ranging from basic life preserving functions like heartbeat, respiration, digestion, over physical and mental work, growth of the body during adolescence, all the way to production of heat in the context of thermoregulation. All tissues vary to some degree in their rate of energy usage, though with skeletal muscle the range is exceptionally large, since it is dependent on the amount of physical work done. [7], [8]

Now, the aforementioned energy stores are filled either by ways of food intake or by transformation of one type of macromolecule into another. Amino acids, either ingested or from muscle protein breakdown, are mostly used to synthesize structural and functional proteins, but also to be directly oxidized, or to be transformed into glucose during gluconeogenesis. Carbohydrates are one of the two main energy suppliers. They are broken down for energy via glycolysis or stored as glycogen in liver or muscle cells. Excess carbohydrates can be transformed into fatty acids via acetyl-Coenzyme A and stored as triacylglycerides (TAGs), which is one way they biochemically contribute to the development of obesity. Nutritional fats are digested and can then be directly used for energy via beta-oxidation of the fatty acids or transformation into ketone bodies, they can be used as building blocks for cell membranes and hormones, or they can be stored as TAGs in the form of white adipose tissue. These are the most important long-term energy reservoir. An average person has approximately 180.000 kcal stored in this way [11], which is a

cushion big enough to enable us to spend our time doing more than searching for food and eating.

Instead of storing TAGs for later use for energy, they, together with glucose, are burnt for heat production by the so-called brown adipose tissue. Developed from the same stem cells as muscle cells, brown AT comes from the mesoderm, and its name derives from the cellular architecture, with not one single, large lipid droplet, but several, and a way higher number of mitochondria, which are with their iron content responsible for the color [12]. It is located only in specific sites throughout the body, like the like in between the shoulder blades, paravertebrally, in the shoulders, and the neck. It is designed for non-shivering thermogenesis and was therefore an important factor for the evolutionary success of the mammals. Until as recently as ten to fifteen years ago it was believed to play no significant role in the adult human, but this view has changed after several studies within this timeframe showed, among other things, relevant activation of brown fat in adults, particularly in relation to cold exposure. Also, in recent years it has been suggested to have and studied in relation to potential health benefits on different organ system, like the cardiovascular, the gastrointestinal, and even the musculoskeletal system [13]. As relevant as its role may be to our health and functioning, however, for this thesis it is not, and from now on “adipose tissue”, “fat”, “fatty tissue”, “bodyfat”, and similar terms exclusively refer to white adipose tissue.

Within the white AT, the TAGs are stored mostly in the form of subcutaneous adipose tissue (SAT), visceral adipose tissue (VAT), or intermuscular adipose tissue (IMAT), at ratios dependent on factors like sex and various endocrinological, metabolic, and genetic factors, some of which influence the metabolism to favor the storage in the latter two forms, like, e.g., (systemically or locally) heightened glucocorticoid levels [14] or increased systemic inflammation [15].

On another note, concerning terminology, the use of the term “adipose tissue” makes more sense compared to calling it “fat” or “fatty tissue”, since it is composed not only of proper adipocytes (fat cells), which make up about 80-90 % of the volume and 20–40% of the number of cells. The remaining tissue is composed of fibroblasts, blood vessels, blood, cells of the immune system, and nerve tissue [12] [16].

Furthermore, AT is not only a form of stored energy and a player in its own regulation, but a major endocrine organ: On the one hand it can be regulated by the

central nervous system and by endocrine signals, but on the other hand it also sends signals out itself. Among these are signal proteins are called adipokines, which include leptin, adiponectin, plasminogen activator inhibitor-1, and hundreds more [17], but also proteins of the renin-angiotensin system, complement components, tumor necrosis factor alpha, and resistin. AT is also involved in metabolism of sexual hormones like estrogen, and glucocorticoids. The degree of impact the endocrine function of AT has is shown by the extent of the negative consequences of both adipose tissue excess and deficiency on the functioning of the whole body, and especially metabolism [18].

1.1.2 Regulation of fat storage and development of obesity

Fat, either coming from carbohydrates or nutritional fat, is stored in the body only when there is excess energy in the system. This is called positive energy balance [9]. During childhood and adolescence this is necessary (to a certain extent) to be able to grow, but if it is maintained over a prolonged timeframe during adulthood it leads to weight gain and possibly obesity. The higher the energy surplus and the longer it lasts, the more pronounced the weight gain. The World Health Organisation (WHO) defines normal, over-, and underweight via the body mass index (BMI), which is calculated as bodyweight in kilograms (kg) divided by height in meters squared (m^2). The range for normal weight lies between 18.50 kg/m^2 and 24.99 kg/m^2. Everything below that is underweight, 25-29.99 kg/m^2 is defined as overweight or preobesity, and 30 kg/m^2 and upward is defined as obesity. Then, there is further division into the subcategories mildly underweight (17-18.49 kg/m^2), moderately underweight (16-16.99 kg/m^2), and severely underweight (<16 kg/m^2) on the low end, and obesity grade I (30-34.99 kg/m^2), grade II (35-39.99 kg/m^2), and grade III (>40 kg/m^2) on the high end [11].

Bodyweight, or to be more precise, the amount of fat stored in the body is regulated by several mechanisms which in turn are influenced by many factors, some of which are genetic and some environmental. [7], [8]

The genetic component seems to account for 40 - 50 % of the interindividual variability in body weight. However, this influence varies strongly depending on weight class. Among the normal-weight population, it accounts for about 30 %,

whereas in obese and severe obese people the genetic component seems to amount to about 60-80 %. The distribution of AT also underlies significant genetic influence ranging from 30 - 55 %. A minimum of 15 genes are causally related to monogenic obesity, and the majority of them is related to the leptin-melanocortin-pathway, which again underscores the importance of leptin with regards to bodyweight and -fat regulation [19].

Concerning environmental factors, a fairly popular review from the year 2006 specified ten more possible antecedents to the rise in obesity: "(1) insufficient sleep, (2) endocrine disruptors (environmental pollutants that interfere with lipid metabolism), (3) decreased variability in ambient temperature, (4) decreased rates of smoking, because smoking suppresses appetite, (5) increased use of medications that can cause weight gain (e.g., atypical antipsychotics), (6) proportional increases in ethnic and age groups that tend to be heavier, (7) pregnancy at a later age (which may cause susceptibility to obesity in children), (8) epigenetic risk factors passed on generationally, (9) natural selection for higher BMI, and (10) assortative mating leading to increased concentration of obesity risk factors (this would increase the number of obese people by increasing population variance in weight)." [20]

The recognition of the substantial genetic influence and societal factors like easily accessible, hyper-palatable, cheap food, increased reliance on machines for transportation, mechanized manufacturing, poor coverage of the importance of diet and movement within the education system, and deliberate promotion and distribution of unhealthy foods due to corporate interests, plus, possibly some of the above-mentioned ten factors on the development of obesity constitutes very important progress, since it can lead to a more well-rounded approach to confronting the obesity epidemic than only applying to individual responsibility, possibly even in a judgmental way.

For all physiological mechanisms concerning the amount of food taken in, the hypothalamus is the central regulator, with the N. ventromedialis acting as the "satiety center" and the lateral hypothalamus as the "feeding center" [7]. While there are many messenger substances involved in short-term regulation of energy uptake via regulation of appetite (e.g., ghrelin, cholecystokinin, insulin), the lipostasis

mechanism seems to play the biggest role in long-term regulation [21]. The amount of stored fat is “communicated” to the hypothalamus by the amount of Leptin released from AT – these two factors are directly proportional to each other – and via a feedback loop the fat mass is kept constant. For each individual, by ways of molecular and neuroanatomic presets, a setpoint for bodyfat is determined, which can also change over time [22]. The mechanisms behind that change are poorly understood, but seem to involve genetic, epigenetic, developmental, and environmental influences [23]. This setpoint is biologically defended by means of manipulating energy balance (the difference between energy uptake and expenditure) by affecting appetite, thyroid hormone levels, sympathetic nervous system activation, and physical movement. This way, further weight loss is hampered and regain of lost weight is favored, so that the amount of body fat stays at this setpoint [23]. This is the case for normal-weight individuals, as well as for obese individuals [24]. And not only weight loss, but also weight gain is defended against in lean individuals that are overfed [25], and even in obese individuals [26], as long as the body fat setpoint stays the same. [7], [8]

The aforementioned Leptin seems to be a major player in these control circuits [27]. It is a hormone that is produced by adipocytes, and its plasma concentration is directly proportional to the fat cell mass. So again, if the fat stores are full, the hypothalamus senses this and in turn reduces food intake and increases energy expenditure. If stored fat is low, the opposite occurs. Most obese individuals show leptin levels that are significantly increased and even disproportionally high for their increased bodyweight. This suggests that obesity is connected to some form of resistance of the tissues to leptin, though the exact role (causal or instrumental?) of this supposed leptin resistance is unclear. [28], [29]

Also, the well-known peptide hormone insulin plays a major role in the regulation of adipose tissue. Macronutrient intake influences insulin levels, with carbohydrates raising levels the most, and this in turn drives glucose and fatty acids into the AT depots and keeps it there [30]. Still, macronutrient intake has yet to be convincingly shown to cause differences in body composition, if provided in an isocaloric manner [31]. Furthermore, insulin influences levels of circulating macronutrients, the release of fat out of AT, signaling of energy status to components of the feeding circuitry, and many other processes. But even though it seems like we have a deep

understanding of the hormone, the extent of insulin's role in the development of obesity is still not totally clear.

However, if the complex system of body fat regulation is hijacked by factors like hyperpalatable, calorie dense foods, the potential comfort of modernity, and to little focus of public policy on educating and incentivizing citizens in the direction of a healthier lifestyle, and thereby an energy surplus is maintained over time, the circuits go awry and the amount of stored bodyfat increases, which leads to the development of disease.

1.1.3 Obesity and chronic disease

Having one's weight sit at least within striking distance of the normal range throughout one's lifetime is crucial for longevity. Of course, there are individual differences concerning a person's ideal weight, and BMI is an imperfect measure too, since it fails to take into account what the value of the number above the fraction line is composed of (e.g. AT vs. muscle tissue), meaning that an individual person can have a BMI a slightly above or below the normal range and be perfectly healthy, but also that an individual can be (metabolically) unhealthy while having their BMI be normal. However, in general it must be stated that being outside of the normal weight range is strongly associated with negative health outcomes [7] [8] [32] (except if it is upwards of the normal range and the underlying cause is not adipose tissue but extra skeletal muscle mass, which is, up to a point, strongly associated with positive health outcomes [33]).

On the lower end, anorexic people (BMI < 18.5) must deal with plenty of physical consequences concerning all large organ systems in a myriad of ways. In general, medical complications of anorexia nervosa are a direct result of weight loss and malnutrition. Starvation induces protein and fat catabolism that leads to loss of cellular volume and function, resulting in adverse effects on, and atrophy of, the heart, brain, liver, intestines, kidneys, and muscles. And that does not even mention the psychological suffering leading to and resulting from it. [34]

A BMI upwards of the normal range is intertwined with just as many acute and chronic health problems. Most of the common chronic conditions such as kidney disease, osteoarthritis, cancer, diabetes, sleep apnea, nonalcoholic fatty liver

disease (NAFLD), gallbladder disease, depression, hypertension, and most importantly, CVD, are directly related to obesity [35], and the most important and mostly strongly BMI-associated of them will be discussed in more detail below.

Also, when talking about mortality, there is a strong connection between obesity and the chance of dying from CVD and cancer, and a significantly increased all-cause mortality [35] [36] [37]. Studies found a J- to U-shaped association of BMI to expected years of life lost (YLL). The maximum YLL for white men aged 20 to 30 with severe obesity, meaning a BMI > 45 kg/m², might lose as much as 8 to 13 years of their life, which is up to a 22% reduction in expected remaining life span, calculated off of average life expectancy [38]. So, the Obesity Society came to the conclusion that overall, there is a causal relationship between obesity and reduced function, reduced quality of life, serious disease, and heightened mortality [39].

The mechanisms behind the relationship of overweight and obesity to morbidity and mortality seem to heavily involve the immune system and a process or rather a state called meta inflammation, which is a low-grade but chronically active state of inflammation involving both the innate and the adaptive part of the immune system [40] Meta-inflammation does not lead to any of the cardinal symptoms of inflammation (redness, heat, swelling, pain, reduced function), even though there are increased pro-inflammatory factors in the circulation and the immune system is active, meaning it is subclinical. Nonetheless, over time it can lead to severe problems throughout all major organ systems.

In chapter 1.1.2 it was mentioned that AT is an endocrine organ, but it was shown that evolutionarily it also functions as an immune organ, playing an important role in maintaining metabolic homeostasis. Obesity suppresses this function, because the functioning of the immune system is affected by excess fat accumulation within the AT. This excess fat can also lead to insulin resistance, and insulin resistance again has been linked to meta-inflammation [40].

Furthermore, obesity seems to create hypoxic conditions within adipocytes by ways of them expanding, and therefore decreasing the blood flow to surrounding adipocytes. Therefore, they must shift to an anaerobic metabolism, which stimulates inflammation via macrophages. On top of that, overfilling of the AT also seems to increase the rate of classically activated M1 macrophages within AT, which

stimulate inflammation, and decrease the rate of alternatively activated M2 macrophages, which would lower inflammation [41].

Also, excess adiposity is one of the most important determinants of adipokines and inflammatory factors associated with coronary plaque rupture [42].

1.1.3.1 Cardiovascular disease (CVD)

As alluded to before, obesity is an independent risk factor for cardiovascular disease (CVD), which has been known for decades at this point. CVD includes coronary heart disease, pectoral angina, myocardial infarction (MCI), congestive heart failure, stroke, hypertension, and atrial fibrillation. Over the last decades a large body of high-quality research has accumulated to confirm the association.

Studies including many thousands of participants looked at CVD, and many of them specifically at the role of obesity in its development, and also at the connection between CVD, obesity, and other risk factors such as diabetes. In [43] it was shown that over three decades the lifetime-risk of suffering from CVD in women and men, all with diabetes, which already increases the risk substantially, was even higher in the obese (78.8% in women, 86.9 % in men) vs. in the normal-weight (54.8 % in women, 78.6 % in men) group.

In another prospective study [44] following more than 7000 British men for 20 years it was shown that major CVD developed at a significantly higher rate in obese (24.9/1000) vs. in non-obese (13.9/1000) subjects. A noteworthy piece of data coming from the study, apart from the clear association between CVD and overweight and obesity, concerns the effect of weight loss. It significantly decreased the risk for developing diabetes mellitus, but not for CVD, except in severely overweight young men. The authors therefore concluded that the longer and the more severely someone suffers from obesity, the more the positive effects of weight loss on the cardiovascular system are limited. In concordance with this, [38] showed that for a given degree of overweight or obesity a younger person, on average, had more YLL (“expected number of years of life lost”, according to the calculation model used in this study) than an older person with the same degree, suggesting that not only the degree of overweight or obesity matters, but also how long a person walks around with it.

The task of evaluating the consequences of obesity on not only manifest, but also subclinical CVD (determined via coronary artery calcium, carotid artery intimal medial thickness, and left ventricular mass), which mostly will be problematic in the long-term, was undertaken by the researchers behind the Multiethnic Study of Atherosclerosis [45]. They included just short of 7000 participants, who were free of manifest CVD at the baseline examination. In white, African American, and Hispanic populations the rate of overweight (60-85 %) and obesity (30-50 %) was higher than in Chinese Americans (33 % overweight, 5 % obese). However, in all of these populations a strong association between obesity and hypertension, coronary artery calcium, an arteria carotis interna (ACI) intimal-medial-thickness over the 80th percentile, arteria carotis communis (ACC) intimal-medial-thickness over the 80th percentile and left ventricular mass over the 80th percentile was shown, despite the higher rate of medication with antihypertensive and/or antidiabetic drugs. Even after adjusting for other well-known risk factors for CVD, such as high systolic blood pressure, high LDL, low HDL, high TAGs, diabetes mellitus, and smoking, the associations persisted.

Also concerning the heart, earlier incidence of non-ST-segment-elevated myocardial infarction (NSTEMI) shows a strong, inverse linear relationship with BMI. The first NSTEMI can occur, depending on the degree of obesity, up to 12 years earlier [42].

Furthermore, atrial fibrillation was shown to appear at a higher rate in overweight and obese individuals [46]. After following people for over a decade (mean follow-up: 13.7 years), about 10 % developed atrial fibrillation. With BMI having been evaluated as both a continuous and a categorical (< 25, 25-30, < 30 kg/m²) variable, a 4 % increased risk for the occurrence of atrial fibrillation per 1 unit increase in BMI was detected, after correcting for other cardiovascular risk factors that is.

High BMI is also associated with hypertension, which in turn is a risk factor for CVD. In a prospective study done in Norway on more than 15.900 women and more than 13.800 men, who did not show CVD or hypertension at baseline, the risk for developing hypertension was 1.4 times higher in subjects whose BMI increased over the duration of the study [47]. One more datapoint concerning the relationship between obesity, hypertension, and diabetes specifically in women was put forward by another large investigation, the Women's Health Study [48]. It included 38.172

non-diabetic, cardiovascularily healthy subjects, and showed that higher blood pressure correlated with higher BMI, and also with older age, a higher prevalence of hypercholesterinaemia, and a family history of diabetes.

1.1.3.2 Diabetes mellitus

Within the same investigation, the Women's Health study [48], where the main outcome measure was time to incidence of type two diabetes mellitus, the mean follow-up time was 10.2 years. After stratifying by BMI, they showed an age-adjusted incidence rate of diabetes among obese women of 7.58/1000 within the normotensive group and 20.53/1000 in the hypertensive group, compared to 0.63/1000 and 2.30/1000 respectively for subjects that were of a normal weight.

In [37] the contribution of the Nurses Health Studies (NHS) I and II to the causes and consequences of obesity were reviewed. Concerning Type II Diabetes, they found that the risk for developing it was at least 3.6 times as high even in the high-normal BMI group (23-23.9 kg/m²) than it was in the low normal BMI group (< 22 kg/m²), let alone the > grade II obese group (BMI > 35 kg/m²), where the relative risk (RR) was 93.2, compared to the low-normal (BMI < 22 kg/m²) group. On the other hand, they also mentioned the positive effect of weight loss, with five or more kilograms lost since age 18 being associated with nearly 50% lower risk.

Among people that already are diabetic, higher bodyweight and especially obesity is associated with poorer blood glucose control, higher blood pressure, and higher cholesterol, and therefore an even higher risk for both macro- and microvascular disease. The American Center for Disease Control (CDC) also looked at people older than 20 years in the U.S.A. who already had a diagnosis of diabetes mellitus type II and explored the connection to overweight and obesity. The results indicated that the majority of people with diagnosed type II diabetes were overweight or obese. Fittingly, losing weight is associated with lower mortality and morbidity among overweight and obese people with diabetes. [49]

Consistent with this observation, several more studies have shown that weight loss is associated with a significantly lowered risk of developing diabetes and lower diabetes-related morbidity and mortality. The aforementioned study of British men [44] also looked at the effect of weight change during a 5-year follow-up, specifically

related to diabetes. It found the relative risk to be 1.76 among the subjects showing a weight gain of at least 10 %, 1.0 among those with stable bodyweight, and a lowered 0.62 among the population that lost weight.

Similarly, the Look AHEAD (Action for Health in Diabetes) study [50] examined over 5100 overweight patients with type 2 diabetes. They compared intensive lifestyle intervention to usual support and education in the form of a randomized trial, and weight loss was connected to improved diabetes control. At the one year mark the intensive lifestyle intervention group had lost 8.6% of body weight, whereas the supportive group had lost 0.7 %. So, the former resulted in clinically significant weight loss in people with type 2 diabetes, and this was associated with better diabetes control, reduced cardiovascular risk factors, and lower use of antidiabetic, antihypertensive, and lipid-lowering medication.

In a large, prospective cohort study in the United States with a 14-year follow-up done on middle-aged women [51] showed that after adjusting for age, BMI was the dominant predictor of risk for incidence of diabetes mellitus type II, and that there is a dose-response-relationship, starting at a high-normal BMI (24 kg/m²). They also looked at weight change as a predictor of risk and got similar results to the research mentioned above. Weight gain above 5 kg was connected to higher risk in a dose-dependent manner, just like weight loss greater than 5 kg was to significantly (ca. 50 %) lower risk. All the results were independent of a family history with diabetes.

These are only a few of many pieces of data showing the strong connection between (the long-term risk of) type 2 diabetes and increasing bodyweight, and, conversely, the lower diabetes-related morbidity and mortality with weight loss. Therefore, encouraging diabetics (and all other patients for that matter) to reach and maintain a bodyweight within the healthy range should absolutely be a priority for all diabetes-care programs.

1.1.3.3 Cancer

Also, many large-scale studies have confirmed a significant association between obesity and cancer. In the repeatedly cited review of the NHS I and II and their follow-up research [37] a correlation between higher BMI as well as increase in BMI

over the lifespan with the development of several types of cancers, among them breast, colorectal, endometrial, ovarian, kidney, pancreatic, and others, is shown.

A prospective study from 2003 [52] followed more than 900.000 Americans who were free from cancer at baseline for a mean 16 years and found a significant association between obesity and cancer. Here once more the degree of overweight or obesity mattered strongly as well. The researchers saw higher rates of death in consequence of cancers in the gastrointestinal tract (esophageal, colorectal, hepatic, gallbladder, pancreatic), the kidneys, and of non-Hodgkin lymphoma and multiple myeloma in proportion to a higher BMI. The subjects with grade III obesity (BMI ≥ 40 kg/m²) showed an overall cancer mortality which was 62% higher in women and 52% higher in men compared to subjects with a normal BMI.

Specifically with breast cancer, not only its chance of occurring, but also of it being fatal is positively connected to bodyweight, to weight gain, and also more specifically to postmenopausal weight gain, while being negatively connected to weight loss [53].

The degree to which high BMI contributes to cancer rates it also shown by [54], where the authors estimate 30% of all colon cancer cases to be attributable to overweight and obesity.

1.1.3.4 Other

Above normal bodyweight also affects the musculoskeletal system. Obesity is directly connected to osteoarthritis, most strongly in the knee joint [55], but also in the hip. Since osteoarthritis has a strong negative impact on patient's quality of life, this consequence of obesity and the importance of weight loss as a preventive and therapeutic measure must be acknowledged.

Furthermore, obesity has been recognized as a strong predictor for non-alcoholic fatty liver disease (NAFLD) [56], and just like in CVD, diabetes, and osteoarthritis, weight loss is beneficial for a lower risk of developing, and a higher chance of benign course of the disease [57].

Apart from the liver, other components of the gastrointestinal system also suffer under the weight of obesity, like the gallbladder, the pancreas, and the colon, and so does the psyche, since obesity has not only biological, but also substantial social

and psychological consequences, often leading to depression and other mental ailments [58].

1.1.4 Body fat distribution and chronic disease

Thanks to the research conducted over the last decades we have come to know that not only the overall amount of adipose tissue within a person's body, but also its distribution over the compartments (visceral, subcutaneous, intermuscular) influences if, how quickly, and which type of disease is most likely going to form.

The relationship between morbidity and mortality and excessive amounts of SAT is a looser one, compared to the one with VAT [59]. Therefore, the ratio between the amount of visceral and subcutaneous abdominal adipose tissue (VAT-SAT-ratio) can serve an important function as a predictor of cardiometabolic risk, risk for cardiac events, and all-cause mortality [60] [61], which shows the importance of accurately measuring it. If this could be done more easily, the inclusion of obesity phenotypes (e.g., visceral metabolic or non-visceral "benign" obesity) into risk profiles that are up to now based on blood pressure, blood lipid levels, age, sex, etc., would be a great improvement [45].

Research in this direction has been going on for a while, but over the last decade it became ever clearer that the fat stored in the form of intermuscular adipose tissue (IMAT) and intramyocellular lipids (IMCL) acts in a similar way within the body as VAT, in the sense that it is, per unit more so than SAT, complicit in furthering metabolic dysfunction, for example via promoting insulin resistance [15]. In the case of IMAT this is happening especially in muscle cells.

Several mechanisms seem to be involved in the comparatively higher morbidity with VAT and IMAT, like a higher contribution to an inflammatory milieu, and insulin resistance [62]. The accumulation of excess fat within abdominal adipose tissue is associated closer with meta-inflammation [41].

A popular hypothesis first put forward by Björntorp in 1992 [63] is the "portal free fatty acid" hypothesis. It tries to explain the destructive hyperglycemic, hyperinsulinemic, hypertriglyceridemic state related to visceral obesity via a dysfunctional liver metabolism. This is proposed to be the consequence of

heightened rate of free fatty acids in the portal circulation, which is itself the consequence of the increased lipolysis (due to insulin resistance and therefore resistance to its antilipolytic effects) in the visceral fat depot. However, in the years since then it has been shown that a large part of the free fatty acids within the portal circulation does not originate from the VAT [64], so this hypothesis can only be a part of the story. [65]

Another part of it is related to insulin resistance. It has been suggested that molecules released by the VAT might contribute significantly to its emergence. Those molecules could be the free fatty acids, as alluded to before, just like pro-inflammatory compounds produced in and released from VAT, like TNF alpha, the interleukins 1 and 6, or resistin. A reduction in adiponectin levels could also be involved since this has been shown before to be connected to lower sensitivity to insulin. [65] [66]

Accumulation of excess VAT could also be indicating dysfunctional adipose tissue which is not able to store the excess energy as it should. According to this model - the lipid overflow model – it is in the end determined by the individual body's ability to deal with excess calories coming from overeating, not moving enough, or both, whether the person develops features of the metabolic syndrome [65] [67]. The metabolic syndrome is a condition composed of the four factors (especially abdominal) obesity (BMI > 30 kg/m²), hypertension (RR > 140/90), dyslipidemia (lowered HDL, increased TG) and insulin resistance/diabetes mellitus type 2 [68]. Research suggests that if the excess calories are taken up by non-insulin-resistant SAT which can expand, metabolic syndrome is unlikely to develop, despite a positive energy balance. If the AT is in any way dysfunctional however (e.g., insulin resistant), the development of ectopic fat deposits is highly likely to happen. These can be located around the viscera, in the liver, around the heart, or within skeletal muscle tissue [67].

This ectopic AT around and within muscles, a compartment similar in size to that of VAT in many people [69], needs clarification around its terminology [15], [35]. In parts of the literature the acronym IMAT is being used to represent int*er*muscular adipose tissue, at other times it is used for int*ra*muscular AT, involving the combination of extramyocellular lipids (EMCL) and intramyocellular lipids (IMCL). IMCL is composed of lipid droplets within muscle cells, which are increased in insulin

resistant, obese people, but also in world class endurance athletes, which indicates that they are not in all cases associated with harm to the individual [70]. Here, “IMAT” will be used for int*er*muscular AT, containing the AT in between different muscle groups and within the muscle fascia, as well as larger accumulations of EMCL within the muscle tissue. IMAT has been shown to rival VAT as an independent risk factor for cardiovascular disease [71], insulin resistance, and type 2 diabetes melllitus, metabolic dysfunction, inflammation, decreased muscle strength, quality, and activation, decreased mobility, higher risk for hip fracture, and more [15]. Therefore, it is important to be able to accurately measure it in order to have another factor helping in identifying individuals at risk for these conditions. So far, the literature shows that this is best done by MRI, which seems to quantify it most accurately, and without the dangers posed by ionic radiation [72].

The accumulation of visceral, but also generally ectopic fat, is furthered by many factors. Several of those have been identified, for example smoking, genetic susceptibility, and neuroendocrine factors [65]. The latter include for example increased activation of the hypothalamus-pituitary-adrenal-axis (HPA-axis), and therefore increased levels of cortisol. The hormone has been known for a long time to influence body fat distribution, favoring the deposition along the trunk, and especially around the viscera [14].

The implications of the effects of visceral adiposity have been examined in numerous large, high-quality studies by now. The IDEA study from the year 2007 [73] looked more specifically at abdominal obesity by factoring in waist circumference in addition to BMI, and evaluated the connection to CVD and diabetes mellitus in 168.000 primary care patients from 63 countries, including Austria. Of all the participants, 27 % of the women and 24 % of the men were obese, with an additional 30 % of women and 40 % of men being overweight. A waist circumference greater than normal (over 102 cm in men and over 88 cm in women, as defined by the National Cholesterol Education Programme (NCEP)) was present in 48 % of women and 29 % of men. CVD was present in 13 % of the women and 16% of the men, and diabetes mellitus in 11 % of the women and 13 % of the men. Their statistical analysis shows a significant increment in the rate of CVD and diabetes mellitus with both increasing BMI and waist circumference. The relationship to CVD and diabetes mellitus is undisputable in both cases, but its strength is even greater

with waist circumference. Interestingly, this interrelation is detectable even in normal weight patients.

Within the aforementioned Multiethnic Study of Atherosclerosis [45], waist circumference was also recorded. However, the authors used BMI as the measure for obesity of their data analysis, which obviously makes sense with the WHO definition being based on it. They did not comment on waist circumference specifically, apart from mentioning it in the same breath with BMI and thereby suggesting that the two measures are tightly correlated. Still, it might be inferred from looking at the study in detail that waist circumference is at least as good at predicting the risk for CVD.

Another study [37] also found waist circumference or waist-hip-ratio to be an independent predictor of the risk for developing diabetes mellitus, with higher waist-hip-ratios (> 0.88) posing up to three times the risk of lower (< 0.72) ones. The same was found for the waist circumference, with an up to six times greater risk with a circumference greater than 96.5 cm compared to under 71 cm.

Another ethnic group that has received attention recently is the Asian population, which appears to be more prone to visceral adipose tissue deposition at lower BMI values.91 This factor could contribute to the explanation, at least in part, of why Asians may be more susceptible to developing type 2 diabetes mellitus at lower BMI values than whites [74].

Also, it was concluded before [75] that associations between fitness (inversely) and BMI directly) to the non-alcoholic fatty liver disease (NAFLD) grow stronger when visceral obesity is included in the statistical analysis.

1.2 Methods for fat quantification

As established in chapter 1.1, due to its role in energy metabolism, energy storage, and as an endocrine organ, AT plays an essential role in human functioning, physiologically and psychologically, and excessive amounts of bodyfat lead to increased risk for lower quality of life, disease, and death. Also, within the basic molecular components of the human body (water, fat, proteins, and minerals), the AT component shows the greatest variability in between, as well as within individual

humans. So, firstly to establish a baseline, and secondly to assess the efficacy of intervention programs over the mid- and long-term [76], it is important to possess accurate and efficient methods for its quantification.

Since the first half of the twentieth century people have experimented with different methods based on a variety of models in order to determine body composition. Then, over the latter half of the last century, a shift took place in the western world from the main problem being a lack of food to it being an excess of food, especially of highly palatable, calorie dense, cheap, and widely available food. This was one of the main factors leading to a rise in the rate of overweight and obesity throughout the population of developed nations, and as an obvious consequence to a rise in obesity-associated disease. All of this furthered the interest in body composition and body fat and its quantification, which led to, among many things, a steep increase in the quality and availability of body composition measurement methods and tools.

1.2.1 Anthropometric tools

The simplest methods rely mainly on anthropometry, like the hip-waist-ratio or the skinfold method. The former one uses the circumference of the waist right in the middle between the lowest rib and the top of the iliac crest and divides it by the circumference of the hips at the widest point of the buttocks with the tape wrapped around horizontally (according to the WHO [77]) to create a ratio which can be used as a proxy for the relationship between the amounts of subcutaneous and visceral AT. Therefore, it can be used as a predictor of cardiovascular health and cardiovascular mortality [78].

The skinfold method relies on a Caliper (a device used to measure the size of whatever is pinched between its tips) to determine the thickness of pinched up skin in defined spots throughout the body. According to the International society for the advancement of kinanthropometry (ISAK) these sites are at the biceps, triceps, subscapular, iliac crest, supraspinale, abdominal, front thigh and the medial calf. The thickness of these skinfolds, together with other measurements like waist circumference, height and weight are then inserted into a formula. This is arguably one of the simplest and most accessible methods, though it is not trivial to use

precisely the right measurement spots in order to make the data comparable and valid [79]. Also, the interobserver-variability is potentially high. [80]

1.2.2 Ultrasound (US)

Ultrasound (US) has also been applied to the assessment of body fat for over half a century. Its underlying principle is the reflection of ultrasonic waves from whichever material the beam interacts with. This beam comes in the shape of short pulses that are sent through the tissue and the returning echo is registered (pulse-echo-technique). Depending on the difference in resistance between two tissue types at their interface, different amounts of sound are reflected. However, US is not as popular a method yet, even though it has some undisputable advantages, like the non-invasiveness, availability, low time cost, and the fact that no damaging radiation is needed. More strong points of US as a tool are its relatively low price, its size and, as a consequence, its portability. With US, body fat is determined by finding certain spots on the body. Those could either be the ISAK spots used in the skinfold method, some of those plus some others, or entirely different ones (depending on the exact method and on the person or team applying it). The spots or areas are then scanned, which means moving the transducer about 5 mm in either direction for spots or moving it across longer distances for areas, like the thigh. The resulting image must be interpreted. Here, several caveats must be mentioned. For one, fascia can be misjudged for an interface between two tissue types, since both appear as uninterrupted white streaks. Interfaces must be interpreted and the two tips of the electronic calipers for measurement must be placed reliably and accurately. This can be done more objectively and comparably the more practice the examiner has had. A partial way around this could be opened up by automatic interface recognition devices which might be commercially available at some point [81]. The determined values for the thickness of the AT layer at the different spots might then be inserted into a formula, which leads right to another area of heterogeneity, since there is an array of different formulas used by different people and gadgets.

Apart from assessing overall body fat percentage, US is also applicable for regional measurements, like in the liver or skeletal muscle. Also, there are methods for

estimating VAT from US measurements, like the abdominal wall fat index for example. It uses the maximum thickness of preperitoneal fat and divides it by the minimum thickness of subcutaneous fat at the abdomen to create a ratio which correlates closely with the ratio of visceral to subcutaneous abdominal fat attained by computed tomography (CT) [82] [83].

However, currently there are no universally agreed upon standards in US measurement of adipose tissue, be it subcutaneous or visceral, be it the pressure of the probe on the site, or the formulas into which the values are inserted. Also, the interobserver variability can be quite high, though the comparability gets better which sufficient practice, as mentioned above. [80] [84] [85] [86]

There have been very promising attempts at standardizing US SAT measurement though. Müller et. al. [87] described their method in their 2015 paper. First, they propose the use of a 3-5 mm thick gel layer to avoid compression of the easily compressible AT. Concerning the settings, high frequencies of 9-18 MHz are recommended for assessing people with very low SAT thickness (e.g., athletes), in order to accomplish a precise depiction of the contours and therefore accurate measurement, since a fraction of a millimeter's difference can change the overall picture quite a bit in subjects with SAT layers spanning only a few millimeters. In obese people with SAT layers measuring several centimeters across for example, an error margin of, e.g., 0.1 mm does not make a relevant difference, so with those subjects the frequency can be lower. The speed of sound in AT with 1450 m/s is slower than in other soft tissues.

After image acquisition, an image segmentation algorithm for the highest possible accuracy in detection of the SAT contour was applied [88]. Following that, the *FAT* software, by rotosport.com, is used for distance evaluation. The software not only determines distance, but also recognizes fibrous structures within the AT and provides the user with distances with fiber included and also excluded.

Since the above mentioned ISAK sites are not ideal for US measurement because they are not providing optimal clarity of image and also require deeper knowledge of and experience with anthropometry, a new set of sites was proposed, that are easily and repeatably detectable. Furthermore, the sites had to fulfill criteria like measurements for finding them having to be relative to the person's height, them being representative of the person's whole body to compensate for individual SAT

distribution patterns, or a uniform SAT thickness pattern in the surrounding area. The proposed sites are located on the upper abdomen (UA), lower abdomen (LA), erector spinae (ES), distal triceps (DT), brachioradialis (BR), front thigh (FT), medial calf (MC), lateral thigh (LT), and an optional site on the external oblique (EO). Not only were the sites carefully selected along the aforementioned criteria, but also the way in which they are measured is highly standardized.

By now, this method has been applied successfully in a range of different subject populations, including obese [89] and anorectic [90] subjects, and athletes like gymnasts and swimmers [87], elite judokas [91], and junior rowers [92]. The interobserver-reliability seems to be very high, given that the examiner is properly trained. Also, no other method can determine SAT layer thickness with the same accuracy. [93] [94]

1.2.3 Bioelectrical impedance analysis (BIA)

A method which poses very little problems in terms of interobserver variability is Bioelectrical impedance analysis (BIA). It works by sending a very small, non-dangerous electrical current through the subjects' body via electrodes most often fixed to the hands/wrists and feet/ankles, in order to measure the electrical resistance and reactance. Water has lower impedance (which is resistance plus reactance) than fat. By the differences in impedance the water content of the whole body can be determined, which can then be used to assess lean body mass (LBM) and, by subtracting LBM from the total body mass, body fat content. To make this work, the body is divided into five cylinder-shaped, fat-free parts (the trunk, two legs, two arms) with AT assumed to be an insulator. On the arms and legs the model of homogenous distribution of AT and water works better than on the abdomen. Still, there are some models which estimate abdominal AT well, but even they cannot be used to differentiate between abdominal SAT and VAT. The models also become more inaccurate with variation in limb length, and they are influenced by the current state of the tissue. Inflamed tissue from e.g., preceding exercise or the hormonal or hydrational status of the subject can change the outcome, just as the subject's age, sex, physical activity, and ethnicity change the models having to be used.

The method's benefits lie in its relatively low cost and wide availability. Also, it can distinguish between intra- and extracellular water. Its problems lie in its inability to accurately determine VAT and fat within organs such as the liver or musculature. [80] [95].

1.2.4 Computed tomography (CT)

Computed tomography (CT) as an imaging method that allows three dimensional, high-definition capturing of either the whole body or any parts of it can also be used in research on body composition. It works by applying a quantity of X-ray beams from all sides to the subject to produce cross-sectional images. With a CT scan it is possible to differentiate between visceral and subcutaneous AT compartments, and also to precisely quantify AT within skeletal muscle or the liver, though for very low amounts of liver fatty tissue it is less accurate, which makes it less usable for diagnosis of low stage fatty liver disease [96]. Though it can produce very accurate and broad data, the method has a few downsides, with possibly the biggest being the necessary amounts of ionizing radiation that must be sent through the body of a (in the context of research on body composition often healthy) subject. However, together with magnetic resonance imaging (MRI) CT is considered to be the gold standard, especially when it comes to measuring AT in a circumscribed region, although the soft tissue contrast is superior in MRI. [80] [97]

1.2.5 Dual-energy X-ray absorptiometry (DEXA)

Another method that is very widespread is called dual-energy X-ray absorptiometry (DXA- or DEXA). Throughout the world most larger hospitals possess a DEXA scanner. Its ubiquity in internal medicine and radiology departments is not due to its use in body composition measurement though. Instead, it is the most common tool for measuring bone mineral density (BMD) and therefore diagnosing and observing osteoporosis or osteopenia, for which it is considered the gold standard. A DEXA scanner uses minor doses of ionizing radiation (more specifically X-ray beams) to create data about the density of a subject's bones ("densitometry"). Two X-ray beams with different energy contents are applied. Bone and soft tissue attenuate

the radiation at different levels, the attenuation changes with the energy of the X-ray beams, and also the ratio of the attenuation coefficients changes. Therefore, by using total absorption at the different energy levels it is possible to subtract out the soft tissue share of the absorption, leaving only the bone absorption, from which BMD can be approximated. In much the same way, DEXA scans can be used to calculate AT mass by subtracting out lean body mass and minerals. Though in clinical practice they are more often used for BMD measurement, DEXA scans also play a role, in part due to their wide availability. Also, they are commonly used in research concerning bodyfat distribution, muscle mass, sarcopenia, and the like. A problem that DEXA scans have is that they do not allow for accurate differentiation between SAT and VAT, because the visceral and part of the subcutaneous AT are inseparable within the image. Therefore, the distribution over these two compartments can only be estimated using an anatomical model predicting the diameter of the subcutaneous layer of AT. [80] [98] [99]

1.2.6 Magnetic resonance imaging (MRI)

Magnetic resonance imaging (MRI) is one of the most important and widely used imaging modalities in today's medical landscape. Put simply, an MRI scanner is a big and strong magnet, which sends radio waves through the body. The emitted signals are detected by a radiofrequency receiver, and then translated into an image by a computer. It enables us to acquire images in various anatomical planes without repositioning of the patient. The images can be used for volume-interpolation, multiplanar reconstruction and three-dimensional analysis. More advanced approaches like diffusion, spectroscopy, and perfusion make precise tissue characterization possible, and with functional MRI activity in parts of the brain during certain actions or states can be visualized, contributing significantly to an understanding of the underlying networks. Compared to CT scans and X-ray images, MRI images exhibit superior soft-tissue contrast, which makes it perfectly suitable for the examination of soft tissue-dominant parts of the body. The excellent differentiation between grey and white matter within the central nervous system makes MRI the superior option for many conditions of it, including demyelinating diseases, different forms of dementia, cerebrovascular disease, numerous

infectious diseases, and epilepsy. For imaging of the musculoskeletal system MRI is widely used, especially for the diagnostics of joint disease and injury, spine imaging (e.g. diagnostics of prolapsed discs), and muscle disease and injury. Also, MRI does not use ionizing radiation, which makes it a great tool in general, but especially for studying healthy subjects (e.g. in a research setting) and even children.

Among the disadvantages are the higher cost per imaging session when compared to CT scans. Also, and more importantly, patient comfort can be a matter of contention, since the acquiring time for images is extended, the device is far louder, and the patient must stay in a confining tube under these circumstances. Some patients are excluded from MRI scans due to metal parts within their body, which can cause serious injury to patients and medical staff. On the analysis and interpretation front, the unique artifacts to which MR images are subject must be mentioned. These must be recognized and dealt with. [80] [100] [101]

Concerning fat assessment, with MRI it is possible to measure AT and lean tissue precisely and directly within many compartments of the body, even AT tissue infiltrating organs, to a degree. This is done using fat-water-imaging with prior separation of fat and water via fat suppression techniques.

1.2.6.1 The Dixon technique

One of the most popular of these fat suppression techniques is the one named after the American physicist Thomas Dixon. He was the first to describe it in 1984, and though it was not too popular in its early days, technological advancements in MRI hardware and software helped it evolve to a point where it can comfortably be used in clinical and research scenarios [102].

This MRI sequence aims at completely suppressing fat. To achieve this, it relies on the different magnetic properties of protons in fat and water molecules. The frequencies at which the protons resonate in the two tissues are offset, so at certain times they are out of phase with each other. This aspect is known as chemical shift, and it enables us to distinguish between the two types of tissues.

With the Dixon technique two images are acquired: A conventional in-phase (IP) spin echo image and another one in which water and fat signals are 180° out-of-

phase (OP). From these two images a water-only and a fat-only image can be created, which allows for direct, image-based water and fat quantification.

$$IP = W + F$$

$$OP = W - F$$

W and F are the signal contributions from water and fat, respectively. Water and Fat images can be calculated from IP and OP images with:

$$\tfrac{1}{2}[IP + OP] = \tfrac{1}{2}[(W+F) + (W-F)] = \tfrac{1}{2}[2W] = W \quad \rightarrow \quad \text{Water-only image}$$

and

$$\tfrac{1}{2}[IP - OP] = \tfrac{1}{2}[(W+F) - (W-F)] = \tfrac{1}{2}[2F] = F \quad \rightarrow \quad \text{Fat-only image}$$

So, in contrast to other techniques the suppression of fat happens during postprocessing, not while the images are acquired.

The Dixon method has several advantages over other fat suppression techniques. For one, it provides a more uniform and artefact-resistant fat signal suppression. So, in comparison with techniques such as Fat-Sat/CHESS (**che**mical-**s**hift **s**elective) it can show proper images in areas where there might be an inhomogeneous magnetic field, like close to metallic hardware. Also, Dixon techniques provide a higher signal-to-noise-ratio (SNR) and are applicable together with enhanced T1-weighted sequences, as opposed to, for example, the STIR (short tau inversion recovery) sequence. Other advantages are the possibility of combination with different sequence types (e.g. spin echo, gradient echo, steady state free procession sequences) and weightings (e.g. T1, T2 and proton density), and the provision of images with and without fat suppression in a single recording session. Also, the ability to show the presence of microscopic fat and to quantify the amount of fat gives the technique great potential for even more widespread clinical use in the future. It is already used in that regard, for example in the staging of liver

steatosis, in the quantification of intramuscular AT in disorders of the musculoskeletal system, like Duchenne's muscular dystrophy, but also in neoplastic and non-neoplastic diseases of the blood and bone marrow to detect and quantify bone marrow infiltration by measuring potential reduction in the proportion of fat within the bone marrow.

Dixon's disadvantages involve its reliance on very modern equipment in order for it to function, and the greater image acquisition time, which is about twice as long as with other fat suppression techniques such as CHESS. Also, even though it is less prone to artifacts, large things like metal prosthesis do remain a potential interference factor. Furthermore, there are artifacts which occur distinctively in Dixon images, where in circumscribed areas a substitution of fat and water signal takes place. One way around this problem is the use of multiple echoes. These sequences are known as Dixon 3-point and 6-point sequences, and they need to be used in combination with a specific algorithm to break down fat and water signals. This process is far more complicated than the mere additions and subtractions the Dixon 2-point method utilizes, but it avoids the interchanging of fat and water signals by enhancing the strength of the separation between them. [80] [102] [103] [104] [105] [106]

1.2.6.2 MRI vs. DEXA

An important factor when comparing different techniques is accuracy. In this case the quest for accuracy is complicated by the fact that there is no undisputed basic truth. Though the consensus moves more and more in the direction of tomographic techniques being the gold standard to which non-tomographic methods should be compared to assess their accuracy, the tomographic techniques vary from each other. One way to help with that is via the use of physical models, although these are limited insofar as they leave out the obstacles brought on by anatomical variations, which do occur frequently in real human subjects. Furthermore, not all methods measure the same physical properties. To use the same example as Borga et. al. in their review [80]: When comparing MRI, which measures fat in volume units, to DEXA, which measures fat in weight units, in order to convert one measurement

unit to the other, constant density must be assumed, which might be inaccurate at times. [107]

However, when talking about total body AT and lean tissue (LT), data acquired by DEXA comes reasonably close to MRI data, but less so when looking at VAT. The divergence from the MRI data becomes even greater with increasing VAT volume, so DEXA becomes less useful in that regard in overweight and obese subjects. Also, DEXA is the least accurate when measuring arm AT [76], which is problematic insofar as MRI also becomes less precise here due to a weakening signal in the outer ranges of the image. The big advantage of DEXA is the synchronous acquirement of data about the skeletal system (bone density and mass). [80] [108] [109] [110]

1.2.6.3 MRI vs. US

It must be said that both methods have their advantages and disadvantages. MRI makes it possible to directly measure the volume of AT throughout different compartments of the body, including the visceral AT compartment, with high accuracy. On the contrary, US techniques can only ever indirectly determine the amount of AT within the body, mostly by measuring distances, like the thickness of the subcutaneous AT layer in different spots, and then rely on mathematical ways of deducing AT volumes or percentages from it, which works fine for SAT, but is limited for the determination of VAT, although there are VAT measuring approaches which seem promising [111].

A big advantage of US is its size and portability, and also its low cost, compared to MRI, which has its bigger downsides in these categories.

One of MRI's biggest strengths, the objectivity, reproducibility, and standardization, is one the US technique's greatest limitations, since there is no universally accepted and used measurement technique and the results are highly dependent on the skill and routine of the examiner. Developments in ultrasound devices as well as software designed specifically for assessing body composition could help in mitigating these limitations [81]. Also, there are very promising methods [87] which might aid in reaching higher standardization of body composition assessment via US, and which have proven themselves in different subject populations already (as described in chapter 1.2.2). [84]

1.2.7 Other methods

There is also a spectrum of highly invasive or in vitro techniques for quantifying bodyfat in living persons and also in cadavers, like letting subjects inhale or inject water-accumulating or fat-accumulating substances, or dissecting and chemically analyzing cadavers, but these are way besides the focus of this thesis.

1.3 Fat segmentation

At this point, the gold standard for fat quantification is still the manual segmentation of fat from images created with the Dixon technique on MRI. This process is very lengthy and tedious though. So, especially for research, reliable and user-friendly automated segmentation is urgently needed. However, there are difficulties to be maneuvered, brought on by varying anatomy, tangled structure of the abdominal organs and thus the AT between them, potential organ motion, blood flow and breathing during image acquisition, or weak contrast between SAT and VAT. Also, with most automated segmentation methods the accuracy declines the more obese the subject is.

1.3.1 AI driven segmentation

The use of artificial intelligence (AI) in radiology is a highly topical subject. The discipline is based upon using machines for medical diagnostics and with each new generation the performance is enhanced and consequently the amounts of data created grow larger and larger. Therefore, it becomes ever more important to make use of tools for accelerated analysis and interpretation of this data. Also, this way different patterns and correlations in the data, which could be of assistance in qualification and quantification of disease-promoting factors and more, might be recognized.

Within machine learning, deep learning plays a significant part. Deep neural networks are grounded on the human brain's way of processing inputs. The networks learn to do a job by contemplating specific cases, similar to the way a

human takes information from his daily experiences and draws conclusions from it. This entails that data is needed for the system to learn.

Neural networks have input and output levels, and at least one hidden level containing the “neurons” (processing units) tasked with transforming the incoming data into something that can be utilized by the output layer. The strength of the signal at a link between neurons is determined by the inputs, which are weighted and tallied up in the manner of a linear combination.

Division of labor between the hidden layers is common, with different types of conversions being done on the incoming information by different layers. The direction of the signal goes from the input to the output level, with an activation function at the end, regulating the output amplitude.

The weightings of the inputs as well as the activation function can be altered by learning. The learning process is governed by a rule, stating that it must change and adapt the parameters of the neural network so that the network gets an input which enables it to create a favoured output [112].

In short, deep neural networks recognize patterns in data and use them to work out intricate problems, and especially when it comes to imaging, deep learning performs extraordinarily well. Since the field of radiology collects information from images, it seems obvious to apply it here. So far deep learning has been used successfully in computer-assisted diagnosis, especially in segmentation, but also in medical image detection and in classification, for example.

[112] [113] [114] [115]

1.3.1.1 Different approaches

So far, several automatic and semi-automatic fat segmentation methods, many of them based on shape and intensity characteristics, have been developed and tested. There is fuzzy-clustering [116], which relies on a general model of fat distribution leaning on a gray-level histogram of the image and also includes spatial information. It is applicable both to water-saturated and non-water-saturated MRI images. On top of this model an automated segmentation algorithm using fuzzy c-means clustering is implemented, and then followed by a thresholding step. An

advantage over formerly attempted methods is the consideration of not only full-, but also partial-volume fat voxels, which overall do contain large amounts of fat. The identification of those partial-volume voxels is aided by the aforementioned spatial information included in the model. One potential downside of the method is the neglecting of signal differences from internal organs.

A similar method is known as K-means clustering [117]. Here, a clustering algorithm is first applied to the images in order to distinguish the subject from the background. Next, contours must be defined, which is accomplished by another algorithm that also removes isolated background pixels. Then a region-growing routine is needed, before so-called snakes are applied to designate the inner border of the SAT- and the outer borders of the VAT- and the AAT-areas. A histogram analysis of the intensity of the MRI image is then performed to deduce a local minimum between the lean tissue and adipose tissue peak, so it can serve as a reference. With this reference it can then be determined if the signal intensity of a voxel lies above or below it, with above meaning the voxel is considered to be only AT. With this method, a visual user interface is provided for simplified supervision and manual correction of the segmentation process. If this is brought to use, the method is relatively reliable and accurate, and especially much faster, when compared to manual segmentation.

Over the last few years, fully convolutional neural networks (F-CNNs) have been developed and widely implemented for pixel- or voxel-wise image segmentation. They allow for the exclusion of any preparational techniques, like division of the image into smaller parts, because they automatically do extraction and integration-type steps by which they heighten the quality of the prediction models. The newer types of these softwares, like the SD-net or DenseNet [118] [119], do an even better job in dealing with anatomical variation. Also, they will probably improve the automatic segmentation field even further since they encourage reusability and information circulation across the network.

Relatively recently, a new architecture for two-dimensional F-CNN in the form of the competitive dense fully convolutional neural network (CDFNet) was introduced by Estrada et al. [120]. Its heightened performance is due to a maxout activation unit, which allows for the generation of specialized sub-networks that set out for distinct structures during the training process. This way, the recognition of more complicated

elements is promoted, while simultaneously reducing the quantity of training parameters in comparison to the networks mentioned above. [120]

[112] [113] [114] [115]

1.3.1.1.1 FatSegNet

Based on this CDFNet architecture, Estrada et al. introduced the fully automatic deep learning pipeline FatSegNet in 2019 [121], with the purpose of even more accurate segmentation of abdominal VAT and SAT. It works with Dixon MRI images, and it is supposed to operate in three steps. First, it has to localize the region of interest, i.e. the abdominal area, which it does by implementing models from the aforementioned CDFNet on coronal and sagittal planes in a semantic segmentation approach. Secondly, the abdominal visceral and subcutaneous AT have to be segmented, which is also done by using CDFNet models, but this time on coronal, sagittal, and axial planes. Thirdly, in the manner of a view aggregation step the generated label maps are assembled into a single final segmentation.

With this approach, even though less parameters are necessary, other deep learning systems are outcompeted. The developers had a set of demands which FatSegNet had to meet. For one, it had to be fully automatic. Also, it should only segment the adipose tissue within the abdomen. Thirdly, it had to be resilient against variations in body form, in order to be applicable throughout heterogenous populations. FatSegNet seems to have met all those criteria. It shows very high test-retest reliability, and its applicability throughout a population with highly divers anatomical features, both in terms of absolute fat mass as well as bodyfat distribution, was proven in a large cohort study. [112] [121]

2 Methods

From 2016 to 2017, in a cooperative effort between the department of radiology and the department of biophysics at the Medical University of Graz, imaging data for further investigation concerning amount and distribution of bodyfat was obtained.

The goal of this thesis is to use this imaging data created via the Dixon MRI technique, have it analyzed by the algorithm FatSegNet and in that manner gain some insights into connections between total amount of bodyfat, its distribution over the compartments, anthropometric data, and sex. Also, the data will be compared to data generated from the same MRI measurements using a k-means based segmentation algorithm, and to US bodyfat measurements taken from the same subjects.

It is important to mention that this thesis was done after approval by the ethics committee of the Medical University of Graz (EK (20-295 ex 08/09), Chairperson Prof. Wolfram Müller).

2.1 Subjects

A collective of 115 young, healthy, mostly well-trained women and men was examined. The subjects were duly advised about the nature, course, significance, and implications of the research beforehand, and written informed consent was obtained.

2.2 MRI imaging

The subjects underwent scanning with a three-dimensional 2-point Dixon MRI sequence, using a 3 Tesla scanner (Magnetom PRISMA, Siemens Healthineers, Erlangen) in a supine position. The body coil was used for signal reception. The scan parameters were as follows: acquisition time = 14 s, echo time = 1.24 ms, repetition time TR = 4.66 ms, flip angle = 8.99 degrees, scanning sequence = GR, sequence variant = SP/OSP, Imaging Frequency = 123.25 ms, Number Of Phase Encoding Steps = 201, Percent Phase Field Of View = 72.22, Pixel Bandwidth = 915, Software Version = syngo MR E11, Acquisition Matrix size = 208x288, SAR = 0.55, Photometric Interpretation = MONOCHROME2, Pixel Spacing =

1.3889\1.3889, Window Center Width Explanation = Algo1. For each subject MRI images were recorded in 368 layers of 1.4 mm slice thickness, reaching from the upper thigh to the upper chest area, during one single breath hold with arms laying at the sides.

2.3 US imaging

Furthermore, the subjects were examined via US for the absolute mass as well as percentage of subcutaneous adipose tissue throughout the whole body (both including, as well as excluding, the fibrous structures around the measurement spots). This was done using a standardized method developed for measurement of the SAT layer thickness and, ultimately, bodyfat mass and percentage. A portable B-mode US device with a linear probe, a 3-5 mm thick US gel layer to avoid tissue compression, and high frequencies of 18 MHz were used to assure the highest possible precision of the measurements. The measurements took place on sites (upper abdomen (UA), lower abdomen (LA), erector spinae (ES), distal triceps (DT), brachioradialis (BR), front thigh (FT), medial calf (MC), lateral thigh (LT)) that were carefully selected along criteria like easy and repeatable detectability, being relative to the subject's height, and being representative of a person's whole body, in spite of individual SAT distribution patterns. Furthermore, an image segmentation algorithm and a distance evaluation software were applied in order to further improve accuracy. The method, the rationale behind it, and past successful performances of it are described in further detail in chapter 1.2.2 and in [87].

2.4 Post-processing

For this thesis, the MRI data was examined to determine which area is the most representative in order to quantify the amounts of abdominal SAT and VAT. The considered factors were having as little lung tissue and as little of the pelvic organs as possible skewing the image. Therefore, and because it is easily repeatable, it was decided to consider only the image layers in between the most ventrocranial point of L1 and the most ventrocaudal point of L5 in the sagittal view, which is a region highly similar to the ones used in other work with automated segmentation of

abdominal adipose tissue [121] [122]. Using *RadiAnt DICOM Viewer* for 3D multiplanar reconstruction, for each subject the slice numbers corresponding to the above-mentioned anatomical structures were determined and arranged in an Excel file, together with other data on the subjects, including subject-code, age at the time of measurement, sex, height, weight and BMI. Subsequently, only the slices in between those numbers were converted into two nifti files per subject – one for the fat image and one for the water image - using *Fiji – ImageJ.* Those nifti files were then arranged into a folder structure fit to be fed into the fully automated deep learning pipeline *FatSegNet*.

2.4.1 FatSegNet

The prepared MRI data was then analyzed by FatSegNet. Working on abdominal Dixon MRI, it uses a 2.5 D strategy to segment AAT with high accuracy.

As mentioned briefly in chapter 1.3.1.1.1, the network operates in three steps: At first, the region of interest, in this case the abdominal area in between the most ventrocranial point of L1 and the most ventrocaudal point of L5, is located by two independent CDFNets in the sagittal and the coronal plane, which extract bounding boxes from each predicted label map. These boxes are then aggregated into one final region map. Secondly, within this map three CDFNets, one each for the coronal, sagittal, and axial view, segment the AT. Thirdly, a view aggregation network combines the maps from the first two steps into an ultimate segmentation. The multiplanar approach is put in place in order to help with the recognition of poorly visible structures resulting from imperfect lateral resolution.

The CDFNet architecture [120] was implemented into FatSegNet because its robustness and broad applicability had already been demonstrated in a similarly challenging endeavor [123]. It shows improved learning of small and complex anatomical structures without an increase in the number of necessary parameters. The CDFNet was created by adapting the Dense-U-Net [118] via insertion of maxout activation units. This Dense-U-Net shows the typical architecture with four dense-block encoders, four dense-block decoders and a bottleneck layer, where each dense-block is built on short-range skip-connections between convolutional layers. With this dense connection method, many convolutional layers are piled upon each

other, with the input of one layer being directly connected to the output of the previous layer. Thereby, reusability of features and information distribution are advanced. As presented in 2015 with the introduction of the U-Net [124], classic long-range skip-connections among all encoding and decoding blocks having the same spatial resolution are used to enhance gradient flow and recovery of spatial information. Also, with these CDFNets competitive learning via maxout-activation units, which are simple feed-forward activation functions that pick the maximum value from their inputs, increases the performance significantly [125] by inducing many sub-networks for specific tasks and simultaneously reducing the number of learning parameters.

For managing the two ways of competition within the network that are thereby raised, namely local and global, two architectural blocks are introduced: The Competitive Dense Block (CDB) deals with local competition. It connects maxout activations of all preceding layers as input to the current layer, and the output of the current layer as input to all following layers in the same block, thus creating dense connections. Global competition is handled by a Competitive Un-pooling Block (CUB). The aforementioned long-range skip-connections from all four encoder CDBs feed into the CUB, which transfers features into the respective decoder CDB.

The bottleneck layer inbetween the encoder and decoder pathways is made up by a 2D convolutional layer and a batch normalization. [121]

The view aggregation network unites the probability maps of the CDFNets responsible for the coronal, sagittal, and axial plane with the use of filters (1 x 1 x 1 3 D convolution) and batch normalization, and a concluding softmax layer gives the ultimate prediction probabilities. In comparison to the hard-coded weighting methods that are usually used, such as voting and averaging, this approach weights every view seperately. [121]

The data thus created includes numerical and graphical components. Among the former are height (cm), average circumference (cm), average area (cm^2), total volume (cm^3), SAT volume (cm^3), VAT volume (cm^3), AAT volume (cm^3), VAT/SAT ratio, VAT/AAT ratio, SAT/AAT ratio, and the volume (cm^3) of the water components of the same compartments and their respective ratios. The latter are comprised of control images *[figure 1]* for each subject, which enable the user to visually inspect the data and check for obvious mistakes possibly made by the algorithm, like

missegmentation of arm tissue (even though this should already be prevented by the view aggregation model built into FatSegnet), which could then manually be corrected for. In our case, no mistakes of this sort were found. The generated data was subsequently integrated into the aforementioned Excel file.

Figure 1: FatSegNet control masks

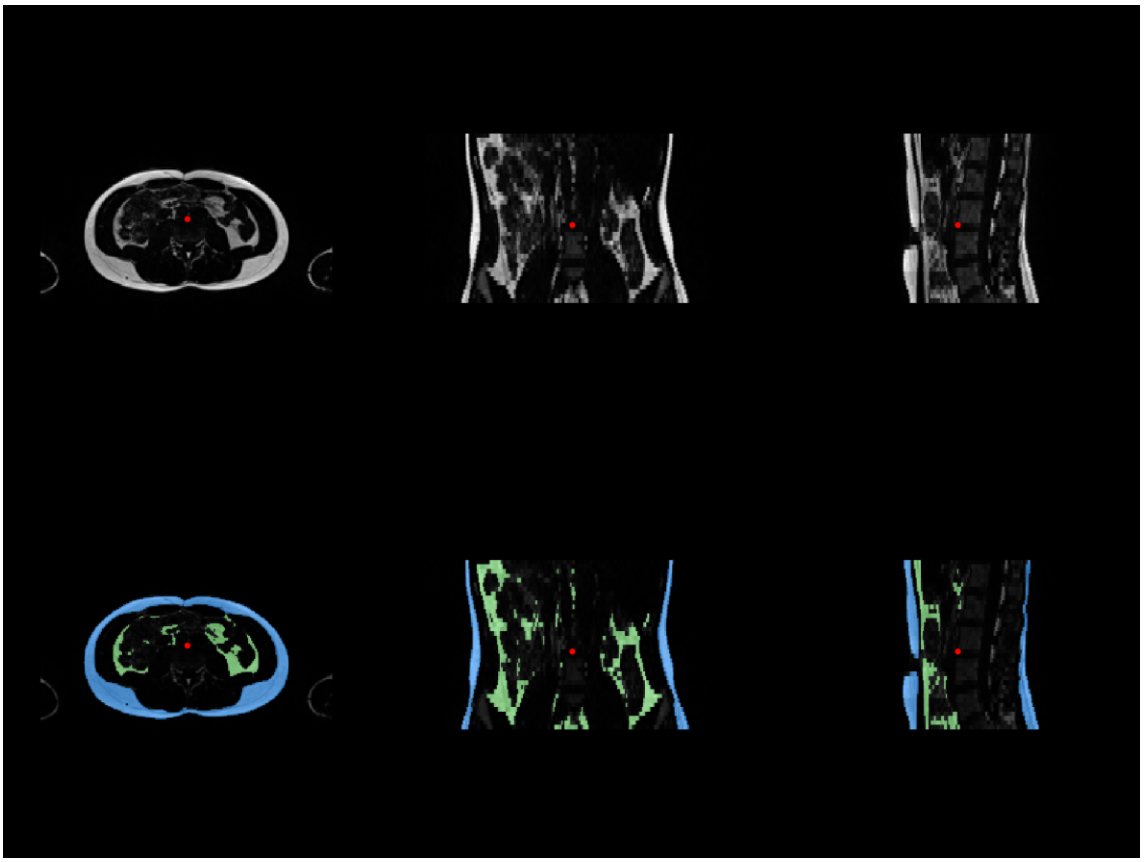

2.4.2 k-means clustering based method

Also, the MRI data were fed into a second algorithm, a k-means-clustering-based method, by a research group from the Gottfried Schatz Research Center's biophysics department, also at the Medical University of Graz. Python was used for the implementation of the algorithm used for SAT and VAT classification. The borders of the SAT compartment were defined by a contour detection algorithm. Thus, a mask of the upper body, excluding the arms, was created. A k-means clustering algorithm [126] was tasked with determining fat and non-fat pixels on the base of fat-only and water-only images. Using the SAT contour pixels as seeds, the SAT area in each slice's fat-only image was seed-filled, with the fat pixels not

contained within the SAT area being assumed to represent VAT. The voxel volume was calculated from the slice thickness and the pixel size, and there was no free space between slices or pixels. The algorithm scanned for outliers too, and corrected 80 of the SAT values, and 112 of the VAT values by linear interpolation.

This same research group had also gathered other data from the subjects, including information about their ethnicity, handedness, preferred sport, training level, weekly training hours, years of training and anthropometric data like their sitting-height, leg-length, mass-index (MI), cormic-index (C), waist-, hip-, bicep-, and thigh-circumference (m), waist-hip-ratio, and waist-sitting-height-ratio.

All this data, together with the outcome of the k-means clustering algorithm's computing of the MRI images, was provided via an Excel file to be partially included into the statistical analysis for this thesis.

2.4.3 Analysis and statistics

The analysis was done using Microsoft Office Excel and IBM SPSS Statistics 27.0. Overall, of the 115 subjects that data was collected from originally, 16 were excluded, since only on the remaining 99 all three measurement methods were correctly and thoroughly performed: Dixon MRI plus fat segmentation via *FatSegNet*, Dixon MRI plus fat segmentation via the k-means based clustering algorithm, and body fat measurement via US. On these 99 subjects, descriptive statistics were applied to display basic information about frequencies, percentiles, minima, maxima, means, standard deviations, and percentages. This was done in numerical and in graphic fashion, using tables, histograms, bar charts, pie charts, and boxplots with fences. Thereafter, it was decided (especially due to the relatively small sample size) that extreme outliers (datapoints beyond a lower outer (Quartile 1 - 3*Interquartile range) or upper outer (Quartile 3 + 3*Interquartile range) fence in the boxplot) were to be excluded, just like subjects with obvious extreme measurement errors with one or more of the three methods. This way, another seven subjects were left out of the final analysis.

Figure 2: Subject selection process

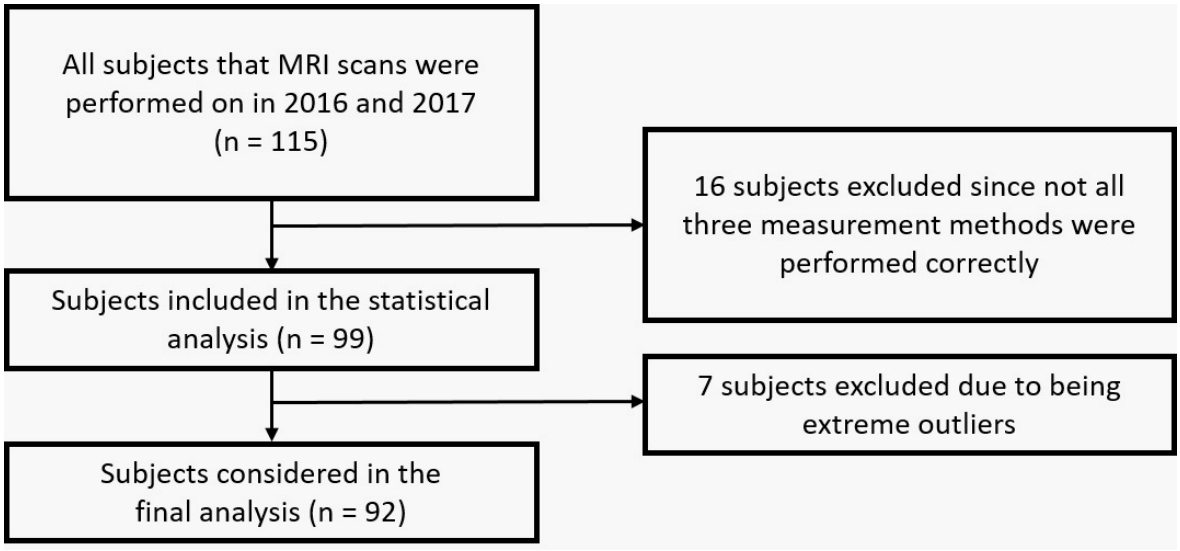

Since it is required for certain tests, normal distribution was tested for. This was done visually via assessment of histograms with included curves, and Q-Q-plots, and mathematically via the Kolmogorov-Smirnov- and Shapiro-Wilk-tests. For comparison of the different variables in the sexes and the measurement methods, t-tests, regression variable diagrams, and bar charts were used. The extent of correlation in metric data was determined via the Pearson correlation coefficient (r), whereas for determination of the correlation between nominal and non-normal metric data the eta coefficient (η^2) was used, which is interpreted as showing the influence of the nominal feature on the metric feature. Also, for further information about the congruency of the measurement methods, the Bland-Altman-method was used. This is a procedure which tries to answer the question if one method of measurement could be replaced by another based on fluctuation [127]. For all tests, two-sided p-values < 0.05 were considered significant.

2.5 Data security

To ensure data privacy, access to the base data was only given at a computer within the department of radiology building, and each patient was anonymized before beginning further analysis of the data.

3 Results

3.1 Demographic data *[Tables 1, 2]*

Of the remaining 92 subjects, 48 (52.2 %) were female and 44 (47.8 %) were male. The average age at baseline was 23.53 years (SD +/- 2.84 years), with the youngest person being 18, the oldest being 36 years old. The male subjects were with 24.02 years (SD +/- 3.02 years) on average just short of one year older than the females with 23.08 years (SD +/- 2.61 years). Most subjects were in their twenties, with 95 % being between the ages of 20 and 28.

The BMI ranged from a minimum of 17.31 kg/m² to a maximum of 28.43 kg/m², with the average being 22.05 kg/m² (SD +/- 2.22 kg/m²). 95 % had a BMI of 26 kg/m² or lower and 89 % lie between 18.5 and 25, meaning that most of the subjects were of a normal weight, going by WHO definitions. Males showed a higher mean BMI than females with 22.97 kg/m² (SD +/- 2.32 kg/m²) versus 21.20 kg/m² (SD +/- 1.74 kg/m²) respectively. The overall minimum and maximum both come from male subjects, whereas the female minimum is 17.62 kg/m² and the female maximum 24.72 kg/m². Concerning percentiles, 95 % of males display a BMI of 27 kg/m² or under, and 86 % lie between 18.5 and 25 kg/m². With females, 95 % of the subjects' BMIs lie in the defined normal range between 18.5 and 25 kg/m². The values for BMI are normally distributed, as confirmed by visual analysis of the histogram and the Q-Q-plot and also via the Kolmogorov-Smirnov- and the Shapiro-Wilk-Tests.

Table 1: Subjects' age

	age overall	**age females**	**age males**
N	92	48	44
mean	23.53	23.08	24.02
SD	2.84	2.61	3.02
min.	18	18	20
max.	36	29	36

Table 2: Subjects' BMI

	BMI overall	BMI females	BMI males
N	92	48	44
mean	22.05	21.20	22.97
SD	2.22	1.74	2.32
min.	17.31	17.62	17.31
max.	28.43	24.72	28.43

3.2 Adipose tissue compartments

The segmentation done via *FatSegNet* and the k-means based clustering algorithm resulted in the following *[Tables 3, 4, 5, 6]* values for the volumes of the VAT, SAT, and AAT compartments, and the VAT-SAT-ratios:

Table 3: Overview of AT volumes and ratios; mean (SD); all volumes in cm³

	FatSegNet				k-means			
	VATvol	**SATvol**	**AATvol**	**VAT/SAT**	**VATvol**	**SATvol**	**AATvol**	**VAT/SAT**
female	289.4 (+/- 135.7)	1709.6 (+/- 564.2)	1999.0 (+/- 654.2)	0.17 (+/- 0.07)	319.5 (+/- 124.8)	1503.0 (+/- 563.4)	1822.5 (+/- 638.7)	0.22 (+/- 0.09)
male	423.4 (+/- 245.5)	1443.8 (+/- 645.1)	1867.2 (+/- 819.0)	0.29 (+/- 0.11)	557.5 (+/- 291.1)	1292.2 (+/- 595.4)	1849.7 (+/- 786.1)	0.46 (+/- 0.16)
overall	353.5 (+/- 206.2)	1582.5 (+/- 615.5)	1936.0 (+/- 736.4)	0.23 (+/- 0.11)	433.3 (+/- 249.7)	1402.2 (+/- 585.4)	1835.5 (+/- 709.1)	0.33 (+/- 0.17)

Table 4: relative frequencies of overall AT volumes and ratios; all volumes in cm³

	FatSegNet				k-means			
	VATvol	**SATvol**	**AATvol**	**VAT/SAT**	**VATvol**	**SATvol**	**AATvol**	**VAT/SAT**
mean	353.5	1582.5	1936.0	0.23	433.3	1402.2	1835.5	0.33
median	301.1	1485.8	1737.2	0.21	376.2	1255.2	1680.1	0.31
SD	206.2	615.5	736.4	0.11	249.7	585.4	709.1	0.17
min.	69.1	665.0	858.9	0.05	106.5	585.6	830.5	0.1
max.	1312.9	3409.6	4194.65	0.61	1731.3	3265.4	4257.7	0.98

Table 5: relative frequencies of female AT volumes and ratios; all volumes in cm³

	FatSegNet				k-means			
	VATvol	**SATvol**	**AATvol**	**VAT/SAT**	**VATvol**	**SATvol**	**AATvol**	**VAT/SAT**
mean	289.4	1709.6	1999.0	0.17	319.5	1503.1	1822.5	0.23
median	265.7	1610.0	1877.9	0.16	293.4	1423.9	1715.6	0.21
SD	135.7	564.2	654.2	0.07	124.8	563.4	638.7	0.09
min.	69.1	756.2	923.0	0.05	106.5	618.2	830.5	0.1
max.	743.0	3093.18	3535.4	0.41	769.2	2948.1	3403.9	0.58

Table 6: relative frequencies of male AT volumes and ratios; all volumes in cm³

	FatSegNet				k-means			
	VATvol	**SATvol**	**AATvol**	**VAT/SAT**	**VATvol**	**SATvol**	**AATvol**	**VAT/SAT**
mean	423.4	1443.8	1867.2	0.30	557.4	1292.2	1849.7	0.46
median	359.5	1213.4	1573.8	0.29	466.4	1084.8	1658.2	0.44
SD	245.5	645.1	819.0	0.11	291.1	595.4	786.1	0.16
min.	177.0	665.0	858.9	0.13	268.2	585.6	938.6	0.14
max.	1312.9	3409.6	4194.7	0.61	1731.3	3265.4	4257.7	0.98

In all compartments and with both algorithms, the minimum and maximum stray relatively far from each other. In the VAT compartment as measured by FatSegNet, the difference is especially large. With 69.1 cm³ vs. 1312.9 cm³, the most voluminous VAT compartment is about 19 times as large as the least voluminous (compared to ca. 5-times larger maximum than minimum each in the SAT and AAT compartment volumes). When sorted by sex, the range shrinks, but the maximum VAT volume still remains 10-times as large as the minimum in females, and 7.5-times as large in males, and the SAT and AAT maxima 4-times as large as the respective minima in females and ca. 5-times in males.

The situation is very similar when measured with the k-means based clustering algorithm: When comparing the largest VAT volume of 1731.3 cm³ to the smallest one with 106.5 cm³, the most voluminous VAT compartment is 16 times as large as the least voluminous, while in the SAT and AAT compartments the maximum volumes are ca. 5-fold the values of the minimum volumes. Here as well, the range decreases after sorting by sex. Still, the maximum VAT volume remains 7-times as large as the minimum in both females and males, and the SAT and AAT maxima 4.5-times as large as the respective minima in females and ca. 5-times in males. So, with FatSegNet the range between the minimum and maximum volumes is slightly larger than with the k-means based method.

Furthermore, the datasets are approaching a normal distribution, but are distinctly skewed towards the minimum. So, the distribution takes the form of the maximum case of an extreme value type I distribution (Gumbel probability density function for the maximum case, *[figures 3, 4]*). The VAT compartments show the highest values for skewness (FatSegNet: 1.970; k-means: 2.563). After sorting by sex, the skewness is slightly lower in females, and even more pronounced in males. Also, most of the VAT volume datapoints measured by either algorithm are scattered tightly around the mean, with less than 5 % of the subjects having VAT volumes exceeding 750 cm³, and less than 25 % having ones exceeding 500 cm³, so the distribution is very peaked, with an extreme upper-tail (Kurtosis: FatSegNet: 5.4; k-means: 9.3). This is less pronounced in females than in males. Concerning the SAT and AAT volumes as measured by FatSegNet, the distribution is far more even in this dimension (kurtosis: 0.3 for SAT; 0.4 for AAT), with the values approaching the bell curve. As measured by the k-means based algorithm, the data are more tail-extreme with the SAT and AAT volumes as well (kurtosis: 0.8 for SAT; 1.2 for AAT).

Figure 3: VAT (A), SAT (B), AAT (C) volume and VAT-SAT-ratio (D) distributions as measured by FatSegNet (FSN)

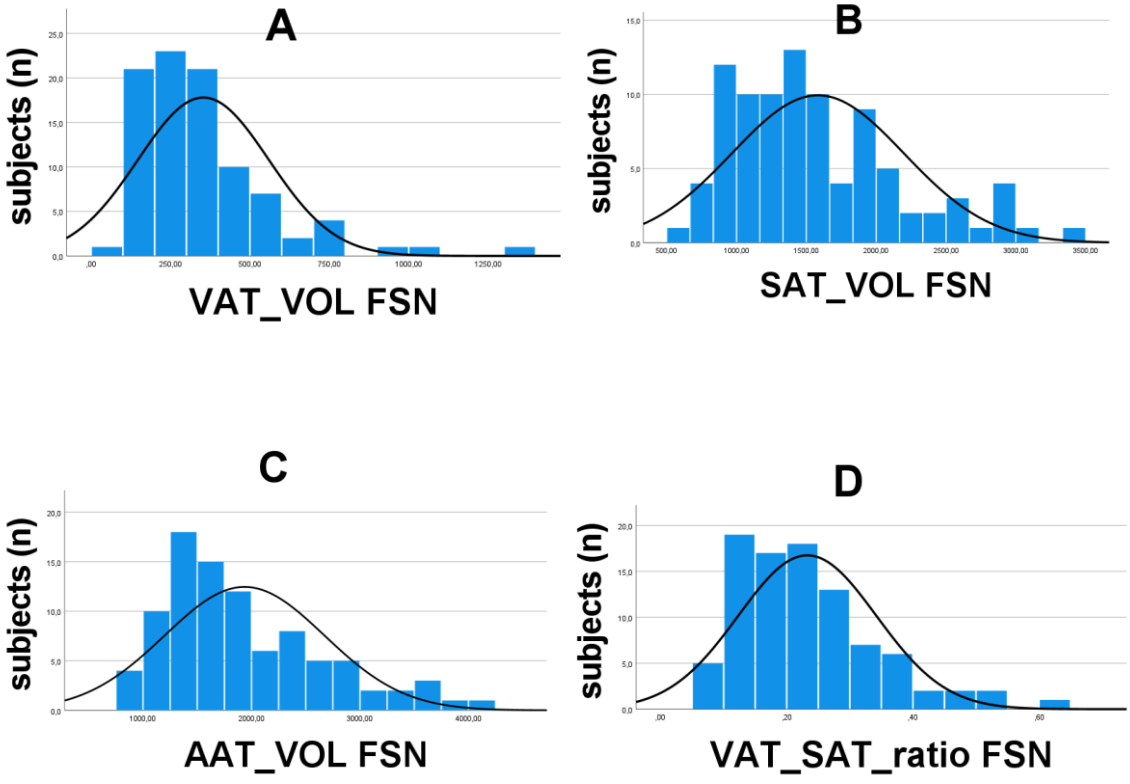

Figure 4: VAT (A), SAT (B), AAT (C) volume and VAT-SAT-ratio (D) distributions as measured by k-means alg.

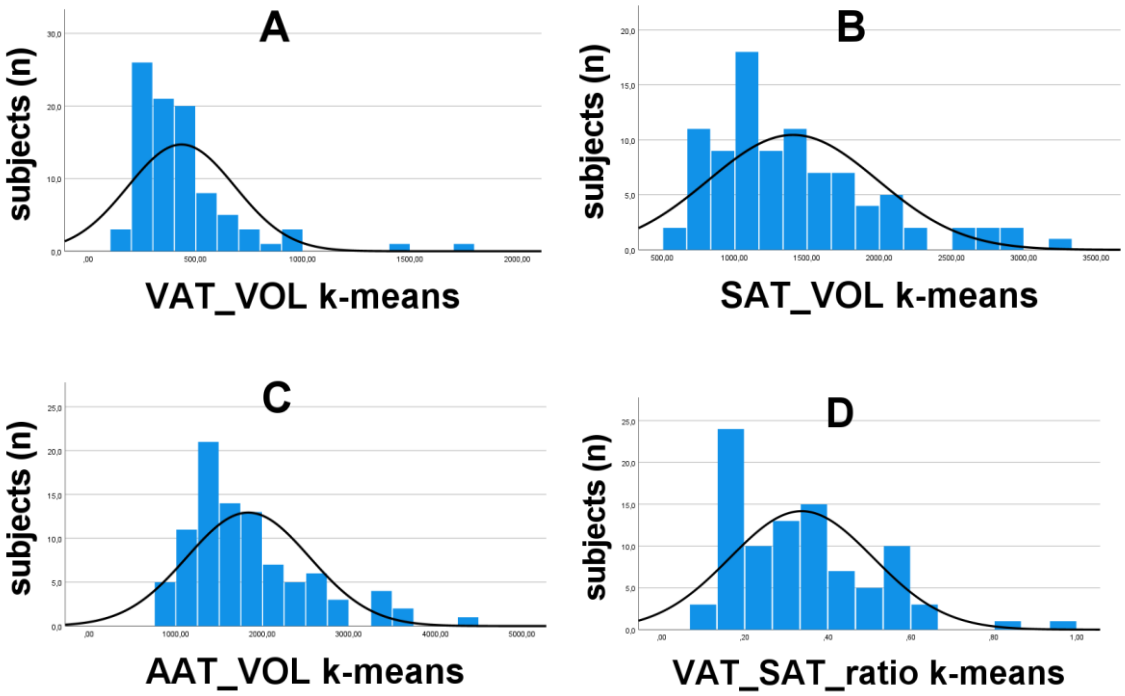

3.3 SAT percentage

The determination of the percentage of subcutaneous fat not just in the abdominal region, but throughout the whole body resulted in the measurements displayed below *[Tables 7 and 8]*. The values were determined in the conventional way, with fibrous structures around and within the AT included (“incl.”), as well as excluded (“excl.”).

Table 7: SAT perc. as measured by US, incl. fibers

	SAT (incl.) overall	SAT (incl.) females	SAT (incl.) males
N	92	48	44
mean	11.2	14.4	7.8
median	11.8	14.4	7.2
SD	4.0	2.1	2.6
min.	3.2	10.0	3.2
max.	20.2	20.2	13.8

Table 8: SAT perc. as measured by US, excl. fibers

	SAT (excl.) overall	SAT (excl.) females	SAT (excl.) males
N	92	48	44
mean	9.9	13.0	6.6
median	10.6	13.0	6.0
SD	3.9	2.1	2.4
min.	2.6	8.9	2.6
max.	18.8	18.8	12.2

The average body fat percentages are 11.2 % (incl.) and 9.9 % (excl.), with the minima at 3.2 % (incl.) and 2.6 % (excl.), the maxima at 20.2 % (incl.) and 18.8 % (excl.), and 95 % of the subjects falling between 4 and 18 % (incl.), respectively between 3 and 16 % (excl.).

Concerning the distribution of the data, the values for SAT percentage are showing two peaks in the histogram *[figures 5, 6]*, with the lower one reflecting the male average (7.8 % incl., 6.6 % excl.) and the higher one reflecting the female average (14.4 % incl., 13.0 % excl.). When sorted by sex, the values for both sexes are distributed normally, once more proven by the Kolmogorov-Smirnov- and Shapiro-Wilk-Tests and graphical analysis of histograms and Q-Q-plots.

Figure 5: SAT perc. (incl.), sorted by sex

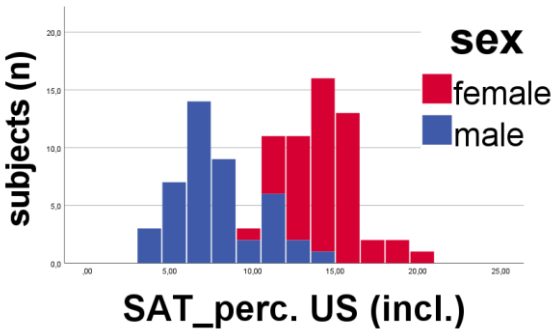

Figure 6: SAT perc. (excl.), sorted by sex

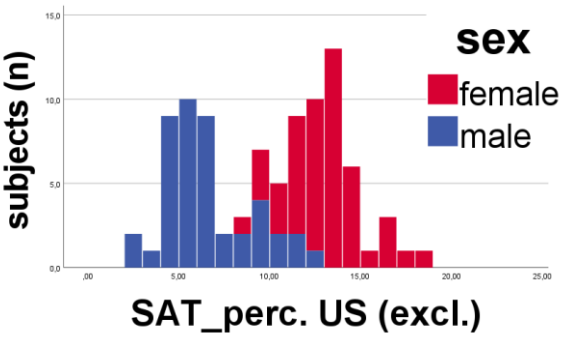

3.4 Sexual dimorphism in body fat-related parameters

Distinct differences between the sexes were observed in most variables. Obviously, the sexes vary in weight and height, which leads to the differences in BMI (T-value: -4.16, p < .001, 95 % CI: (-2.61)-(-0.92)) *[figure 7]*.

Figure 7: BMI differences between the sexes

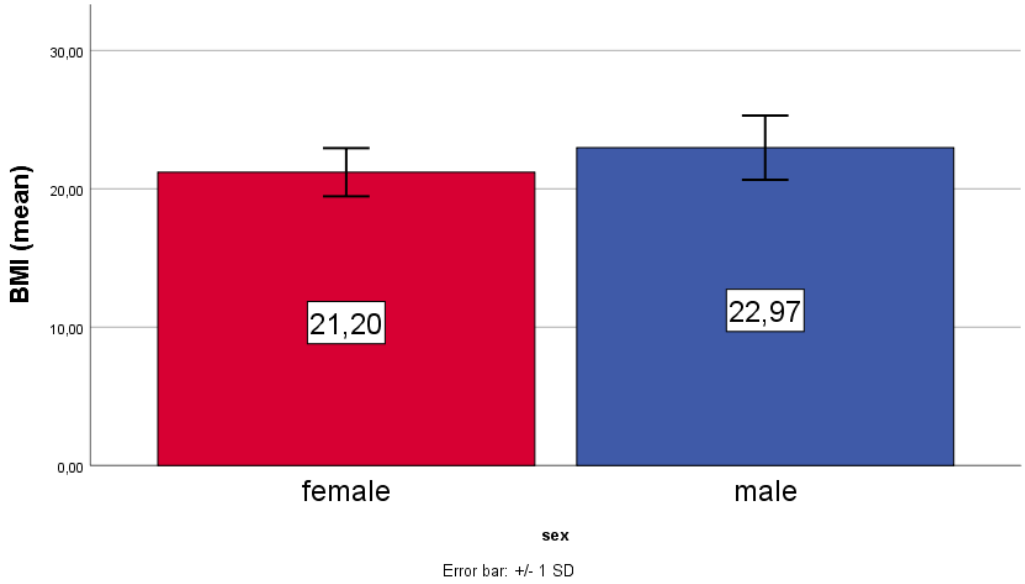

The BMI overall shows a significant correlation to the volume of the abdominal AT (FatSegNet: *r(90) = 0.40, p < 0.001*; k-means alg.: *r(90) = 0.53, p < 0.001*). The correlation is stronger in females than in males, and it is stronger with the SAT (females: *r(46) = 0.66, p < 0.001*; males: *r(42) = 0.40, p = 0.007*) than with the VAT (females: r(46) = 0.339, p = 0.019; males: r(42) = 0.172, p = 0.265) compartment, since with male subjects there is not even a significant correlation between BMI and VAT volume.

3.4.1 Differences in MRI measurements

When looked at seperately in female and male subjects and in the two segmentation algorithms, VAT volume (FatSegNet) on average is higher in males (423.4 cm^3) than in females (289.4 cm^3) ($\eta^2 = 0.326$, p = 0.001), whereas SAT volume (FatSegNet) is higher in females (1709.6 cm^3) than in males (1443.8 cm^3) ($\eta^2 = 0.217$, p = 0.038).

When both these compartment volumes (FatSegNet) are put together in the form of AAT (AAT = VAT + SAT) the aforementioned differences go in the direction of evening each other out, but still the overall absolute mass of AT in the abdominal area is on average higher in females (male avg. = 1867.2 cm³, female avg. = 1999.0 cm³), though the effect size is very small ($\eta^2 = 0.090$, $p = 0.039$) *[figure 8]*. With the k-means clustering based segmentation algorithm *[figure 9]*, the numbers are trending in the same direction, with VAT volume on average being higher in males (557.5 cm³) than in females (319.5 cm³) ($\eta^2 = 0.479$, $p < 0.001$), SAT volume being higher in females (1503.0 cm³) than in males (1292.2 cm³) ($\eta^2 = 0.181$, $p = 0.044$), and both volumes with their differences put together almost cancelling each other out (male avg. = 1849.7 cm³, female avg. = 1822.5 cm³) ($\eta^2 = 0.019$, $p = 0.045$), even though here the females show a slightly higher AAT volume on average.

Figure 8: Differences between the sexes throughout the AT compartment volumes as measured by FatSegNet (FSN)

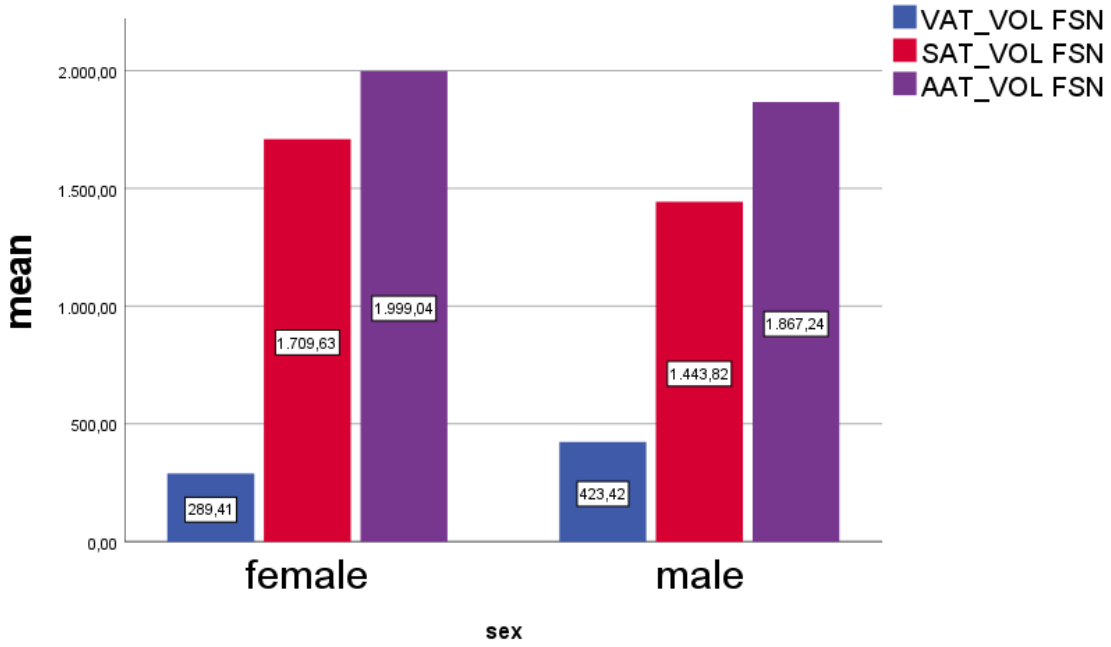

Figure 9: Differences between the sexes throughout the AT compartment volumes as measured by k-means alg.

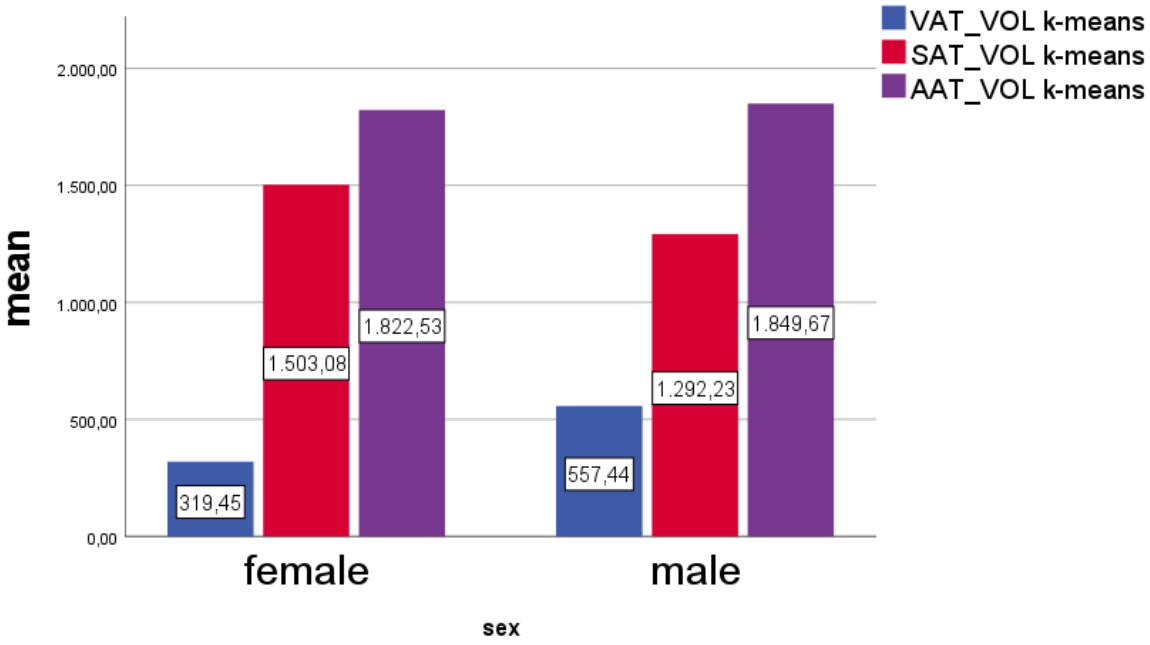

Concerning the VAT-SAT-ratio *[figure 10]*, large and significant differences between the sexes can be observed (FatSegNet: $\eta^2 = 0.566$, $p < 0.001$; k-means: $\eta^2 = 0.660$, $p < 0.001$). The values created by FatSegNet (females: 0.17; males: 0.30) as well as the ones created by the k-means algorithm (females: 0.23; males: 0.46) show a mean VAT-SAT-ratio about twice as high in males compared to females.

Figure 10: Sex differences in the VAT-SAT-ratio as measured by FatSegNet (A) and the k-means alg. (B)

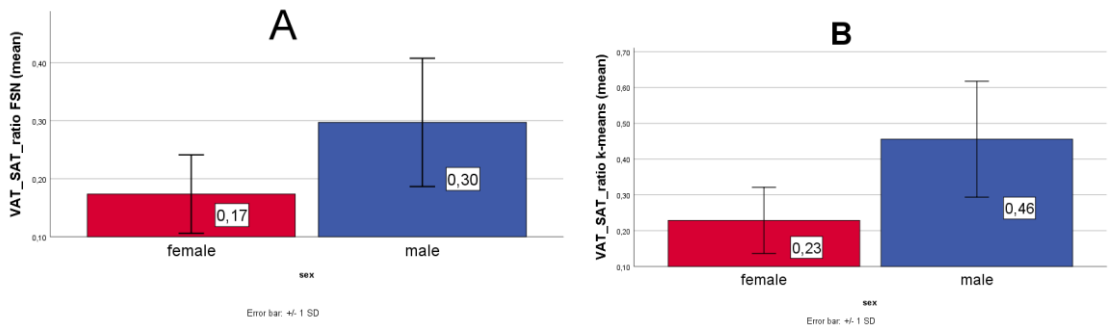

3.4.2 Differences in US measurements

The whole-body SAT percentage as measured by US also shows significant differences (T-test: *SAT perc. (incl.)*: T-value: 13.6, p < 0.001, 95 % CI: 5.65-7.58; *SAT perc. (excl.)*: T-value: 13.6, p < 0.001, 95 % CI: 5.48-7.35) between the sexes (*figure 11*), with the female distribution peaking at higher values (mean SAT perc. incl.: 14.40 %, excl.: 13.00 %) than the male one (mean SAT perc. incl.: 7.78 %, excl.: 6.58 %).

The correlation between BMI and the SAT percentage (incl.) is there - and significant, and very similar in strength in females and males (females: *r(46) = 0.403, p = 0.005*; males: *r(42) = 0.384, p = 0.010*).

Figure 11: Sex differences in the SAT perc. (incl.) (A) and (excl.) (B) as measured by US

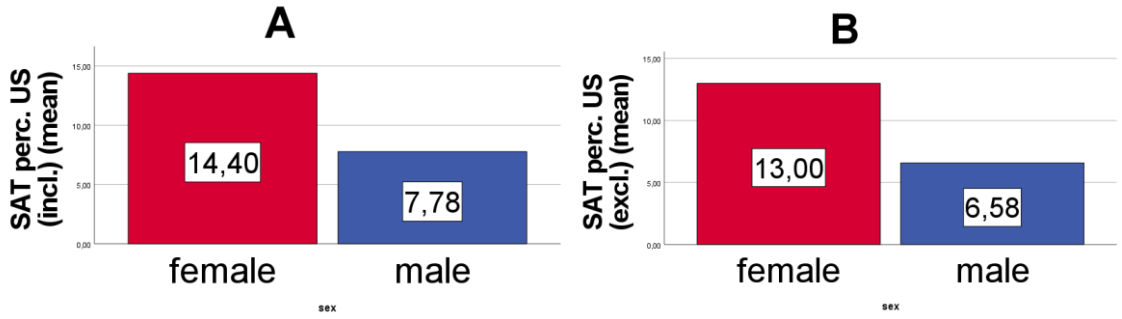

3.5 Comparison of the methods

3.5.1 MRI (FatSegNet vs. k-means based alg.)

The graphical comparison of the data *[figure 12]* created by the two algorithms indicates that they produce, on average, very similar outcomes. Overall, FatSegNet tends to measure lower VAT, higher SAT, and higher overall AAT, compared to the k-means algorithm.

For VAT, SAT, AAT, and the VAT-SAT-ratio there is a strong and significant correlation between the results put out by the two algorithms in both female (VAT: *r(46) = 0.98, p < 0.001*; SAT: *r(46) = 0.98, p < 0.001*; AAT: *r(46) = 0.98, p < 0.001*; VAT-SAT-ratio: *r(46) = 0.94, p < 0.001*) and male (VAT: *r(42) = 0.62, p < 0.001*;

SAT: *r(42) = 0.91, p < 0.001*; AAT: *r(42) = 0.86, p < 0.001*; VAT-SAT-ratio: *r(42) = 0.55, p < 0.001*) subjects, with a stronger correlation in females. This is also shown in the regression variable diagrams. Three subjects (50, 51, 52), all male, are lying distinctly further from the regression line than all others.

Figure 12: Regression variable diagrams showing the relationship between the values for VAT (A = females, B = males), SAT (C = females, D = males), AAT (E = females, F = males), and the VAT-SAT-ratio (G = females, H = males) created by the two algorithm (x-axis = FatSegNet, y-axis = k-means alg.)

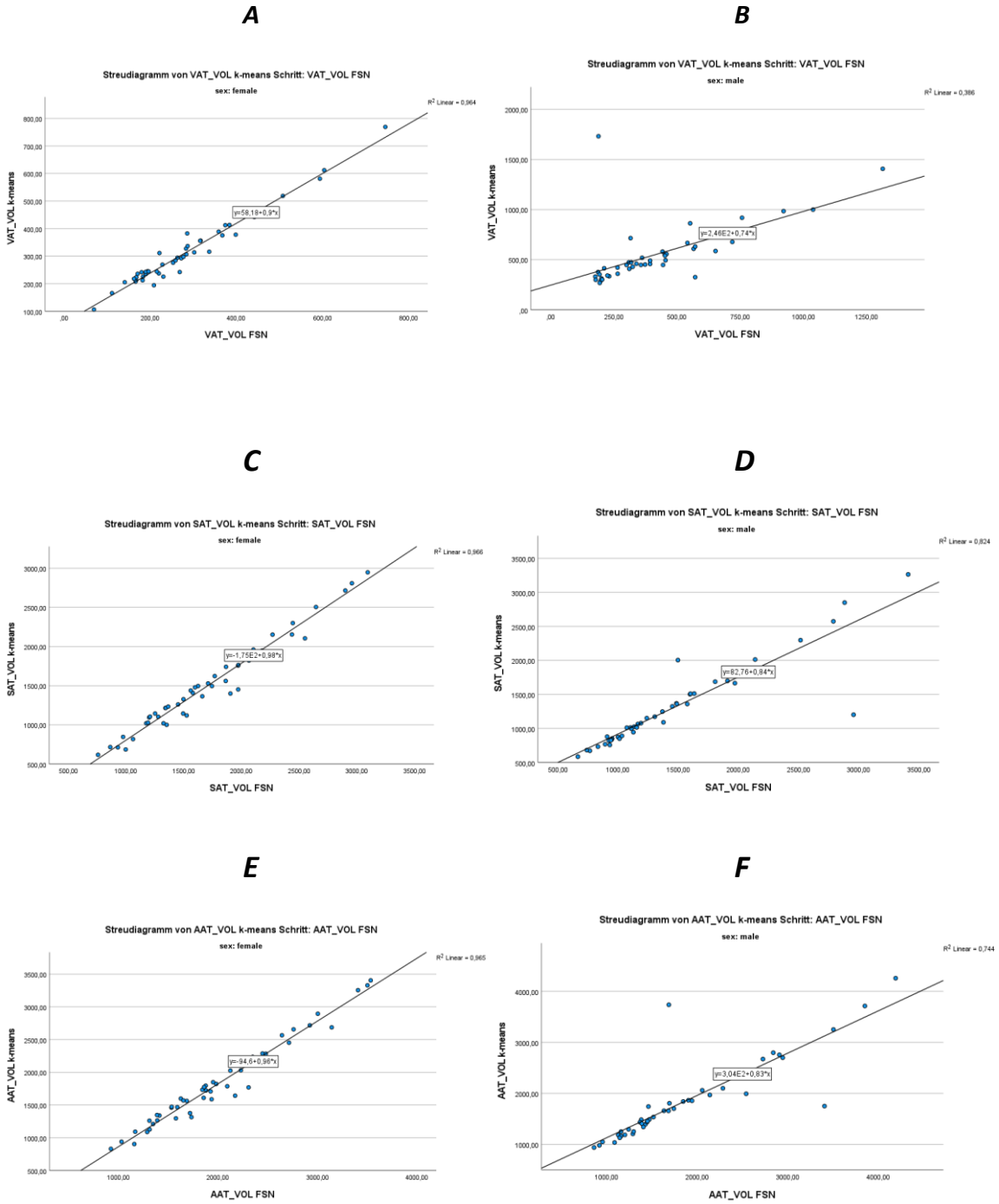

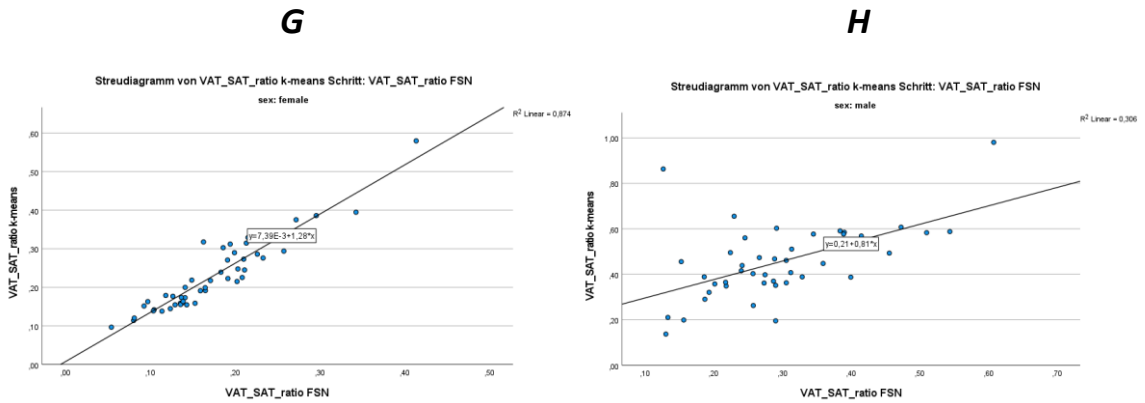

The Bland-Altman-plot also indicates that FatSegNet and the k-means based algorithm get similar results out of the Dixon MRI images, since most of the values for the differences between FatSegNet's and the k-means based algorithm's numbers for VAT, SAT, AAT, and the VAT-SAT-ratio are scattered right around the mean of the differences and lie in between the fences *[figure 13]*. Again, three subjects, the same ones that were mentioned regarding the regression variable diagrams (50, 51, 52), are lying far outside the upper and lower fences.

Figure 13: Bland-Altman-plot for VAT (A), SAT (B), AAT (C); and the VAT-SAT-ratio (D)

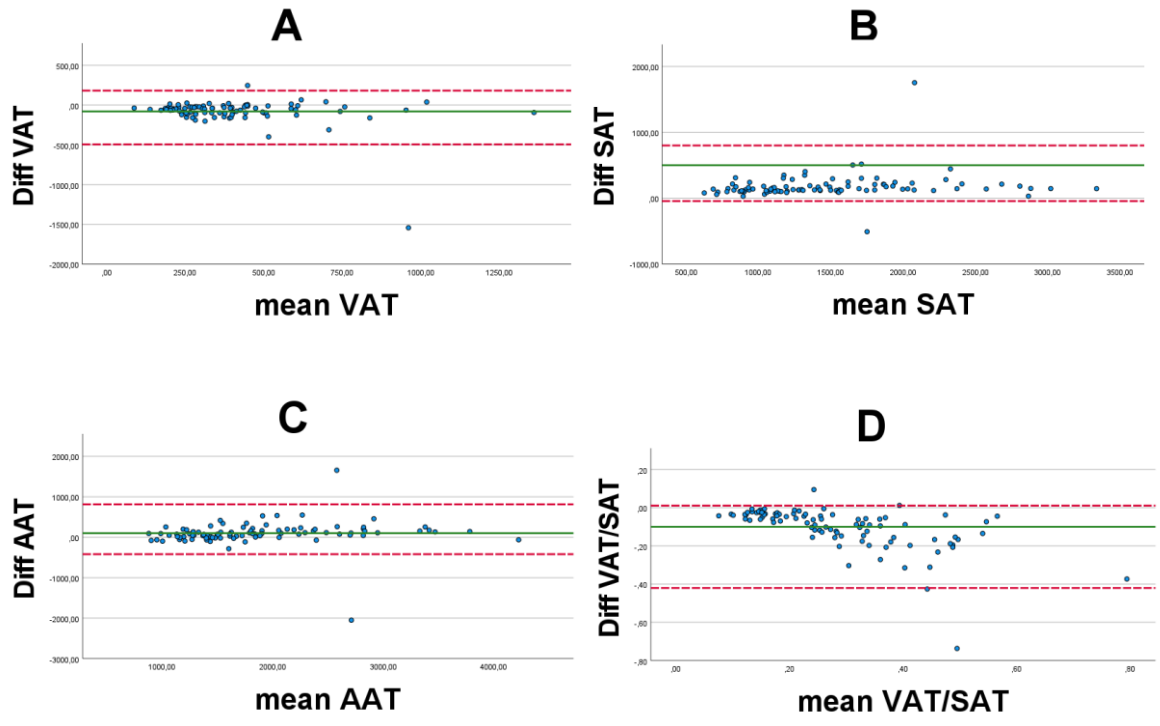

The BMI does not correlate strongly or significantly with the VAT-SAT-ratio measured by either algorithm (FatSegNet: *r(90) = 0.08, p = 0.456*; k-means alg.: *r(90) = 0.05, p = 0.635*).

3.5.2 MRI vs. US

When comparing the MRI based methods to the US measurements, the correlation of the US-measured SAT percentages (incl. and excl. fibers) with the values for the VAT and SAT, as well as the combined AAT compartments is strong and significant with measurements from both algorithms, and in both sexes. In male subjects, the correlation is slightly stronger *[Table 10]* than in female subjects *[Table 9]*. Furthermore, the FatSegNet measurements correlate slightly stronger with the US measurements than the k-means measurements do, especially when it comes to the correlation with the values for the VAT compartments.

Looking at the VAT-SAT-ratios, no clear correlations with the US measurements can be found, only a small trend towards an inverse relationship, but none of the values were shown to be significant.

Table 9: Correlations of US-measured SAT perc. (incl. and excl. fibers) with the measurements from FatSegNet and the k-means alg. in females

	FatSegNet				**k-means alg.**			
	VAT	**SAT**	**AAT**	**VAT/SAT**	**VAT**	**SAT**	**AAT**	**VAT/SAT**
SAT perc. (incl)	r(46) = 0.42, p = 0.003	r(46) = 0.72, p < 0.001	r(46) = 0.71, p < 0.001	r(46) = -0.15, p = 0.294	r(46) = 0.35, p = 0.014	r(46) = 0.67, p < 0.001	r(46) = 0.66, p < 0.001	r(46) = -0.34, p = 0.019
SAT perc. (excl.)	r(46) = 0.43, p = 0.003	r(46) = 0.72, p < 0.001	r(46) = 0.71, p < 0.001	r(46) = -0.15, p = 0.309	r(46) = 0.37, p = 0.011	r(46) = 0.68, p < 0.001	r(46) = 0.67, p < 0.001	r(46) = -0.33, p = 0.021

Table 10: Correlations of US-measured SAT perc. (incl. and excl. fibers) with the measurements from FatSegNet and the k-means alg. in males

	FatSegNet				k-means alg.			
	VAT	**SAT**	**AAT**	**VAT/SAT**	**VAT**	**SAT**	**AAT**	**VAT/SAT**
SAT perc. (incl)	r(42) = 0.62, p < 0.001	r(42) = 0.86, p < 0.001	r(42) = 0.86, p < 0.001	r(42) = 0.007, p = 0.965	r(42) = 0.52, p < 0.001	r(42) = 0.87, p < 0.001	r(42) = 0.85, p < 0.001	r(42) = -0.26, p = 0.092
SAT perc. (excl.)	r(42) = 0.62, p < 0.001	r(42) = 0.86, p < 0.001	r(42) = 0.86, p < 0.001	r(42) = 0.007, p = 0.964	r(42) = 0.52, p < 0.001	r(42) = 0.88, p < 0.001	r(42) = 0.86, p < 0.001	r(42) = -0.26, p = 0.088

The same relationship can be shown in graphical fashion *[Figures 14 and 15]*. The strongest MRI-to-US-measurement relationship as shown in numbers, as well as graphics (the narrowest distribution around the regression line), independent from type of algorithm or sex, exists between the abdominal SAT compartment volumes and the US - SAT percentages.

Figure 14: Regression variable diagrams showing the relationship between the values for SAT perc. US (incl.) and VAT (A = females, B = males), SAT (C = females, D = males), and AAT (E = females, F = males) as measured by FatSegNet

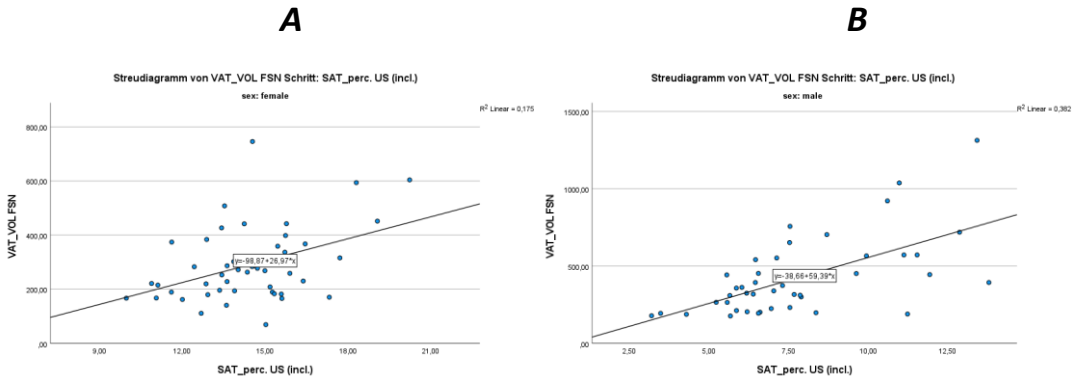

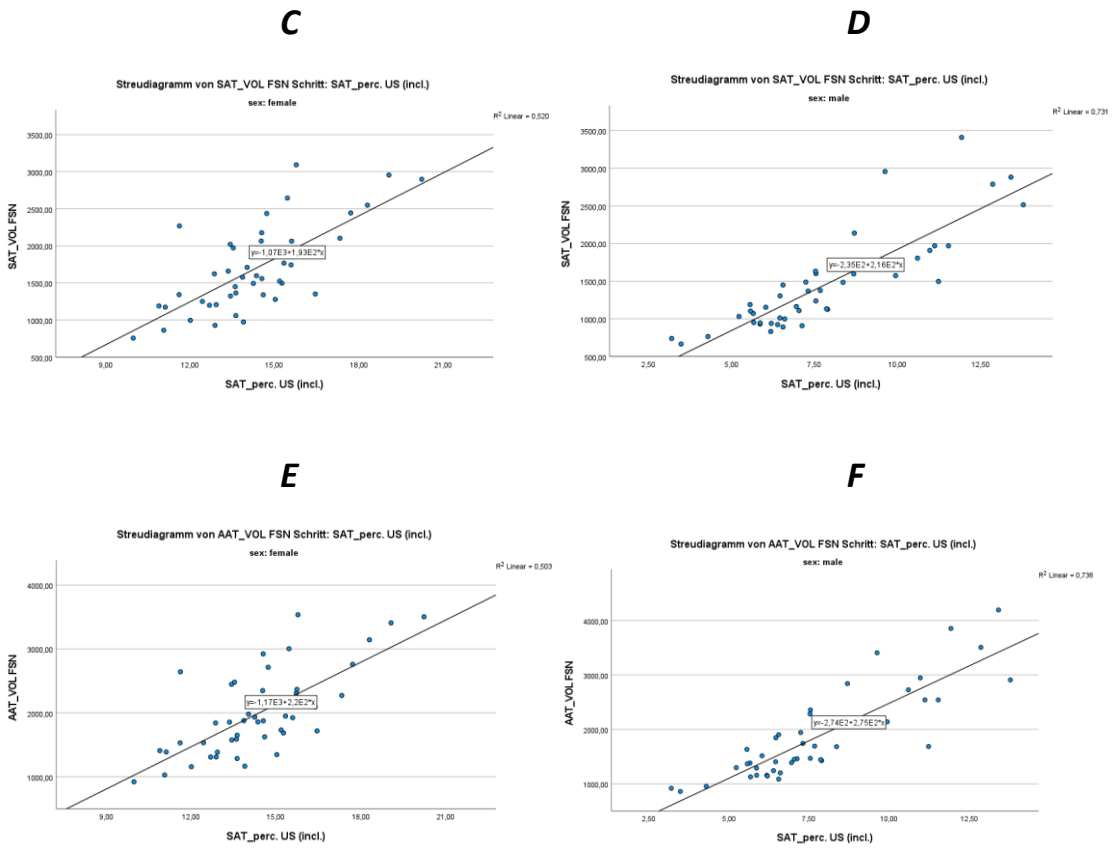

Figure 15: Regression variable diagrams showing the relationship between the values for SAT perc. US (incl.) and VAT (A = females, B = males), SAT (C = females, D = males), and AAT (E = females, F = males) as measured by the k-means alg.

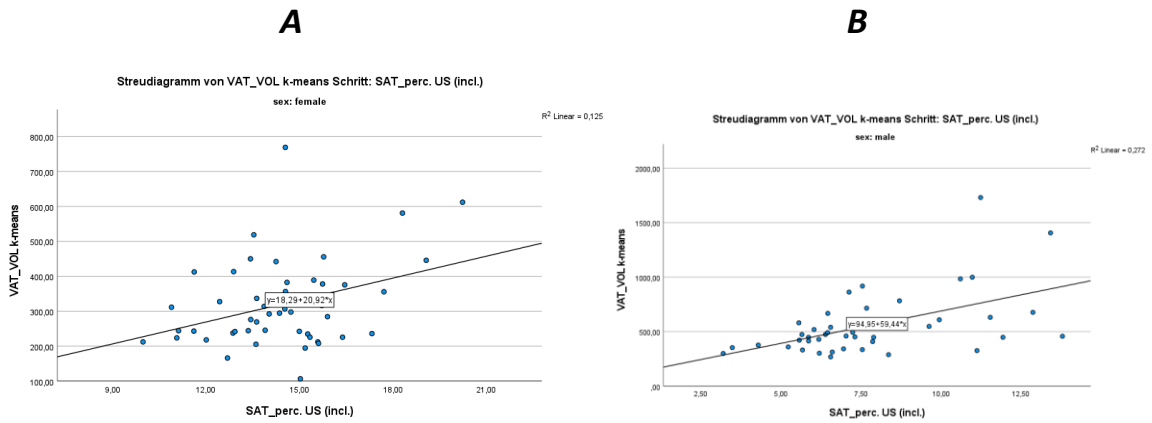

C

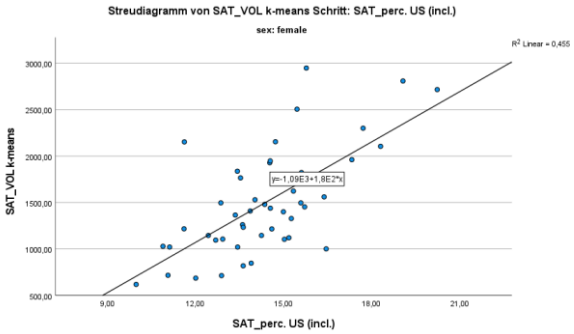
Streudiagramm von SAT_VOL k-means Schritt: SAT_perc. US (incl.)
sex: female
R² Linear = 0,455
y=-1,09E3+1,8E2*x
SAT_VOL k-means
SAT_perc. US (incl.)

D

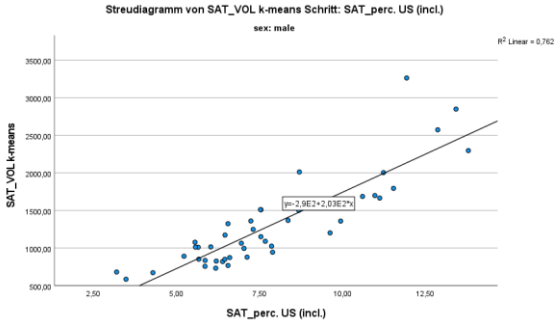
Streudiagramm von SAT_VOL k-means Schritt: SAT_perc. US (incl.)
sex: male
R² Linear = 0,762
y=-2,9E2+2,03E2*x
SAT_VOL k-means
SAT_perc. US (incl.)

E

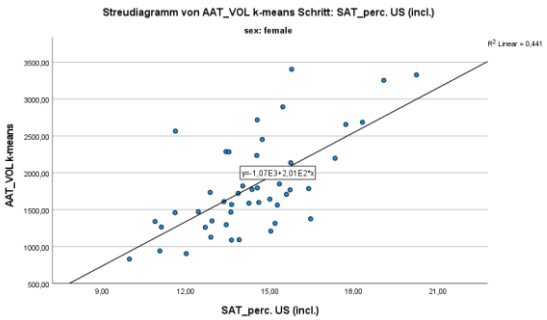
Streudiagramm von AAT_VOL k-means Schritt: SAT_perc. US (incl.)
sex: female
R² Linear = 0,441
y=-1,07E3+2,01E2*x
AAT_VOL k-means
SAT_perc. US (incl.)

F

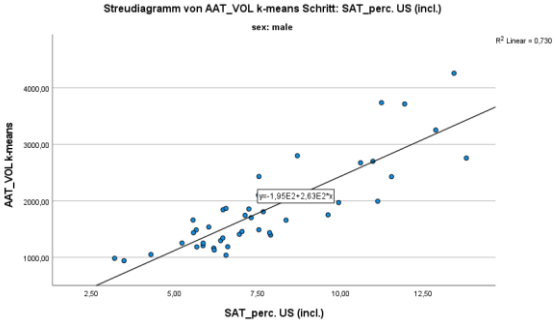
Streudiagramm von AAT_VOL k-means Schritt: SAT_perc. US (incl.)
sex: male
R² Linear = 0,730
y=-1,95E2+2,63E2*x
AAT_VOL k-means
SAT_perc. US (incl.)

4 Discussion

Automatic fat segmentation

Until recently, MRI imaging with fat suppression techniques such as the Dixon technique with subsequent manual segmentation of the AT has been the gold standard when it comes to exact and direct quantification of AT [80] [97] [128]. However, as automatic segmentation methods are becoming more accurate, faster, and easier to use, they increasingly occupy that position [129]. Now it remains to be determined which type of AI algorithm is best suited for this task. However, the existing literature suggests that deep-learning-based neural networks such as FatSegNet are superior in their accuracy, especially when it comes to measuring VAT [113] [121]. This is most likely due to FatSegNets greater ability to deal with the complexity of the anatomy around the abdominal organs and other structures. It owes this to the underlying structure, which facilitates the training of complex tasks via boosting the formation and development of specialized sub-networks targeted – in this case - at specific parts of the anatomy by encouraging local and global competition within the network [120]. Also, FatSegNet is superior in speed (about one minute of computation time for the volume of a whole subject) and adaptability, since it, being based on deep learning, can be retrained and redesigned easily [121]. Our results are in line with the literature in that they show that compared to FatSegNet, our control data acquired via the simpler, more rigid k-means-clustering based method, which relies on pixel clustering, region growing, and active contours (snakes) for the identification of the divisions between the background and the AT compartments within each slice [117] [121], gets slightly deviating values for the amount of AT within a person's abdomen. This overestimation of SAT and more prominently VAT is at least in part due to it (and similar methods) attributing voxels displaying parts of the intestines to fat because their intensity value is often higher than the lean-to-fat threshold, and also due to partial volume effects [117].

Still, our overall results delivered by both methods are very similar. For VAT, SAT, AAT, and the VAT-SAT-ratio there is a strong and significant correlation between the results put out by the two algorithms in both females and males, with stronger correlations in females (see chapter 3.4.1). The Bland-Altman-plot also indicates that FatSegNet and the k-means based algorithm get similar results out of the Dixon

MRI images. However, three subjects (numbers 50, 51, and 52), all male, are lying far outside the upper and lower fences here in the Bland-Altman-plot, as well as distinctly further from the regression line in the regression variable diagrams, compared to all others. In all three of these subjects, one algorithm measures very high values, and the other one measures very low values. The values themselves do not classify as outliers, but the difference between them does. Overall, this indicates measurement errors specifically with these three subjects. However, after manually examining the subjects‘ control images, we could not pin down the error’s source. Though, our most promising hypothesis comes down to the k-means based algorithm having classified gluteal muscle as AT and therefore erroneously showcasing higher values.

SAT measurement via MRI and US

Another important finding of the thesis concerns the strong correlation between the SAT values as determined by MRI measurement with the Dixon technique and application of an AI algorithm for segmentation, and the SAT percentages calculated from US measurements. In our data, the strongest MRI- to US-measurement relationship, independent from type of algorithm or sex, exists between the abdominal SAT compartment volumes and the US - SAT percentages. The segmentation done by FatSegNet correlates slightly stronger with the US measurements than the one done by the k-means algorithm does. This demonstration of accuracy when comparing the US method to the gold standard of MRI plus segmentation [80] further justifies the application of US-based methods using SAT layer thickness measurements plus calculations [87] for the quantification of SAT. This is especially important since the US-based methods are, in addition to sharing one of the main advantages of the MRI-based methods - not using ionizing radiation, a lot cheaper, faster, and easier to use. US devices are, especially compared to an MRI scanner, small in size and easily transportable. However, the US technique’s greatest limitations lie in the areas of reproducibility and standardization, since there is no universally accepted and used measurement technique and the results are highly dependent on the skill and routine of the examiner. Though in this case, with experienced examiners and a sophisticated method [87], the US data holds up very well when compared to the gold standard.

Other research comparing SAT measurements done by US methods to those done by MRI- [130] [131] as well as CT-based methods [132] come to the same conclusions: There is higher inter- and intraobserver reliability in tomographic methods but, especially when also considering their other advantages, the US methods easily hold up well enough to justify their use and especially their further development.

VAT measurement via US

In our data the correlation between *SAT* percentages determined by US and *VAT* volumes determined by MRI plus FatSegNet also turns out to be significant, with the FatSegNet measurements correlating slightly stronger with the US measurements in comparison to the k-means measurements. It might even be strong enough to further justify the use of US-SAT measurement as another proxy for estimating visceral adiposity, especially when other correlates like waist circumference, or waist-hip-ratio are factored in as well. Still, the relationship between US-measured SAT and MRI-measured VAT is of course distorted as a consequence of individual (e.g., sex- or age-related) differences in the distribution of bodyfat over the compartments. However, since there are several methods for determining VAT itself via US, this is the more promising path. The US measurements included in this thesis only measured the SAT percentage, but other research looked at US-based VAT measurement methods and deemed them reliable in comparison to tomographic imaging-based measurement. So far, these methods are based on the abdominal wall fat index (AFI) [133], mesenterial fat thickness (MFT) [134], intra-abdominal fat thickness (IAFT) [135], measurement of peri- and para-renal fat [136], and a few others. So, a fair amount of selection must occur to be able to specify which of the methods are the most reliable, and which ones might be best suited for distinct subject populations, like pregnant women [131]. Of course, MRI makes it possible to directly measure the volume of AT throughout different compartments of the body, including the visceral AT compartment, with higher accuracy, but has its own disadvantages, especially in terms of practicality and cost (see above). Considering those, the US-based methods for assessing visceral adiposity are definitely an area which justifies further development and extended use in the future, especially as the methods become even more reliable.

Sex-related differences in measurement and body fat

When looking at relationships between measurement methods and compartments while stratifying the data by sex, distinct differences between female and male subjects were observed in most variables. Concerning AT compartment volumes, with the FatSegNet segmentation, VAT volume on average is higher in males (423.4 cm^3) than in females (289.4 cm^3), whereas SAT volume is higher in females (1709.6 cm^3) than in males (1443.8 cm^3). With the overall AAT (AAT = VAT + SAT) the aforementioned differences go in the direction of evening each other out, but still the overall absolute mass of AT in the abdominal area is on average higher in females (male avg. = 1867.2 cm^3, female avg. = 1999.0 cm^3). With the k-means clustering based segmentation algorithm the numbers are trending in the same direction. This means the sex differences in compartment volume show up even in absolute numbers. So, when considering them in concordance with female subjects' on average significantly lower body weight, they are even more distinct.

Concerning the VAT-SAT-ratio (a strong predictor of cardiovascular risk and all-cause mortality [60] [61]), large and significant differences between the sexes can be observed. The values created by FatSegNet (females: 0.17; males: 0.30) as well as the ones created by the k-means algorithm (females: 0.23; males: 0.46) show a mean VAT-SAT-ratio about twice as high in males compared to females. Other research found very similar differences with very similar magnitudes, like VAT-SAT-ratios about twice as high in men compared to women [137].

In females, there is overall stronger agreement between the two algorithms when it comes to AT volumes. This might be traced back to the k-means based method's lower accuracy when it comes to segmenting VAT (see two pages above or [117]). Males have, on average, more VAT and less SAT than females, and both algorithms are more in line with each other when measuring SAT compared to measuring VAT. So, in males the compartment in which one of the algorithms (the k-means based one) is more prone to error is, on average, significantly larger. Therefore, the correlation between the results presented by the two algorithms is weaker in males.

The SAT percentages as measured by US also show significant sexual dimorphism, with the female distribution peaking at higher values (mean SAT perc. incl.: 14.40 %, excl.: 13.00 %) than the male one (mean SAT perc. incl.: 7.78 %,

excl.: 6.58 %). This is once more in line with the current understanding that females have, on average, more subcutaneous AT [138].

So overall, concerning sex differences our results line up nicely with the well-established and consensually accepted typical male and female bodyfat distribution patterns [137] [138] [139] [140] [141] [142], with males having relatively more VAT and less AAT, and females on the other hand having relatively more SAT and more AAT, and males therefore having a higher VAT-SAT-ratio.

Subject population and limitations

Concerning specifics of this thesis, it must be said that even though the subjects are very similar in the sense that they are all athletically active young women and men, it is still a relatively heterogenous population concerning their AT-related data. This might be attributable to the fact that there are athletes ranging from long distance runners, who typically have a very low BMI and bodyfat-percentage, all the way to judokas and powerlifters, who have a higher BMI and oftentimes also a higher bodyfat-percentage. Also, the range reaches from recreational/hobby-athletes up to top athletes. Consequently, the volumes of AT within the compartments and the bodyfat-percentages are also very heterogenous, covering a span ranging from very low to high-normal values (e.g., VAT volumes from 69.1 cm^3 up to 1312.9 cm^3 - a 19-fold difference; or SAT-percentages from 3.2 to 20.0 %) compared to healthy adults [143] [144]. After sorting the data by sex, the range between the minima and maxima shrinks, but remains significant, and is overall slightly larger with FatSegNet than with the k-means based method. This also speaks to the fact mentioned in the introduction (chapter 1.2, first paragraph) about AT being the body compartment with the largest inter- and intraindividual variability.

Furthermore, correlation of BMI with total VAT volume is often described to be poor [121], mainly because VAT constitutes a much smaller fraction to total adipose tissue than SAT [145]. With our population this was different, which might be due to the overall volumes of AT being relatively low. In overweight and especially obese people on the other hand, the low correlation between the BMI and VAT volume clearly underlines the need for direct, reliable VAT measurement.

Another noteworthy feature of the subject population concerns the distribution of the data for the AT volumes, which takes the form of the maximum case of an extreme value type I distribution in both sexes and all compartments. This means most subjects lie very close to the mean, but a wider distribution is shown above, compared to below the mean (see chapter 3.2, *[fig. 3.1]* and *[fig. 3.2]*). This means the data are not normally distributed, which had to be expected, since real-valued *random* variables are represented in the form of a normal distribution [146], but the subjects in this study were *not* selected randomly, but instead for being young athletes, so they do not represent the general population. Therefore, most subjects were of an extraordinarily low bodyfat percentage and of a medium BMI (mean BMI 22 kg/m²), a few were very skinny, and almost none were overweight, let alone obese.

On that note, it must be mentioned that this study did not include any severely obese subjects. Consequently, our methods were not tested in this population, though it is one where automatic segmentation algorithms are reported to be more prone to error [147], especially ones that are not deep-learning-based [117]. Concerning FatSegNet however, it can be assumed to perform just as well in severely obese people, since it was tested on subjects up to a BMI of 47.7 kg/m² taken from the Rhineland-Study population [121].

Another point worth mentioning refers to the aforementioned intermuscular adipose tissue (IMAT) (see chapter 1.1.4), which occupies an increasingly important spot in our models for understanding metabolic dysfunction, obesity, different patterns of body fat distribution, as well as the mechanisms leading to and the morbidity resulting from those [15] [62]. With Dixon MRI however, IMAT is not registered, so any imaging and segmentation methods also capable of capturing IMAT might assist in painting an even more comprehensive picture of an individual's risk for future ailment.

4.1 Conclusion

The data acquired via this thesis is congruent with the current literature in showing that a non-deep-learning-based automatic segmentation algorithm, while producing reasonably reliable outcomes when segmenting AT from Dixon MRI images, does

not show the same level of accuracy in measuring abdominal adipose tissue (AAT), especially visceral adipose tissue (VAT), that a deep-learning-based algorithm like FatSegNet does.

Furthermore, we could show that, compared to Dixon MRI plus subsequent AT segmentation, US-based measurement of subcutaneous adipose tissue (SAT) is highly accurate and reliable, especially if done by experienced examiners implementing a sophisticated and highly standardized method.

Lastly, our data is in line with the current understanding of sexual dimorphism in AT distribution patterns, with females having relatively more overall AAT and more SAT, and males having relatively more VAT.

References:

[1] https://www.who.int/news-room/fact-sheets/detail/obesity-and-overweight (accessed on 05.12.21)

[2] Ogden CL, Carroll MD, Kit BK, Flegal KM. *Prevalence of Childhood and Adult Obesity in the United States*, 2011-2012. JAMA. 2014;311(8):806–814. doi:10.1001/jama.2014.732

[3] https://ourworldindata.org/obesity (accessed on 05.12.21)

[4] https://www.hsph.harvard.edu/obesity-prevention-source/obesity-consequences/economic/ (accessed on 29.01.22)

[5] https://www.worldobesity.org/news/world-obesity-day-all-countries-significantly-off-track-to-meet-2025-who-targets-on-obesity#:~:text=Obesity%20also%20has%20staggering%20financial,regions%20%5Bsee%20table%205%5D. (accessed on 29.01.22)

[6] Garthe I, Raastad T, Refsnes PE, Koivisto A, Sundgot-Borgen J. *Effect of two different weight-loss rates on body composition and strength and power-related performance in elite athletes.* Int J Sport Nutr Exerc Metab. 2011 Apr;21(2):97-104. doi: 10.1123/ijsnem.21.2.97. PMID: 21558571.

[7] Pape, H.-C., Kurtz, A., Silbernagl, St., *Physiologie*, 7. Auflage. 2014, Georg Thieme Verlag, Stuttgart.

[8] Silbernagl, St., Lang, F., *Taschenatlas Pathophysiologie*, 5. Auflage. 2018, Georg Thieme Verlag, Stuttgart.

[9] Hill JO, Wyatt HR, Peters JC. *The Importance of Energy Balance.* Eur Endocrinol. 2013;9(2):111-115. doi:10.17925/EE.2013.09.02.111

[10] Felig P, Owen OE, Wahren J, Cahill GF Jr. *Amino acid metabolism during prolonged starvation*. J Clin Invest. 1969 Mar;48(3):584-94. doi: 10.1172/JCI106017. PMID: 5773094; PMCID: PMC535724.

[11] Gallagher D, Heymsfield SB, Heo M, Jebb SA, Murgatroyd PR, Sakamoto Y. *Healthy percentage body fat ranges: an approach for developing guidelines based on body mass index.* Am J Clin Nutr. 2000 Sep;72(3):694-701. doi: 10.1093/ajcn/72.3.694. PMID: 10966886.

[12] Berry DC, Stenesen D, Zeve D, Graff JM. *The developmental origins of adipose tissue.* Development. 2013 Oct;140(19):3939-49. doi: 10.1242/dev.080549. PMID: 24046315; PMCID: PMC3775412.

[13] Cypess, Aaron M., *Reassessing Human Adipose Tissue,* Journal Article, 2022, New England Journal of Medicine, page 768-779, 386/8, 10.1056/NEJMra2032804 [doi]

[14] Mi-Jeong Lee, Pornpoj Pramyothin, Kalypso Karastergiou, Susan K. Fried, *Deconstructing the roles of glucocorticoids in adipose tissue biology and the development of central obesity,* Biochimica et Biophysica Acta (BBA) - Molecular Basis of Disease, Volume 1842, Issue 3, 2014, Pages 473-481, ISSN 0925-4439, https://doi.org/10.1016/j.bbadis.2013.05.029.

[15] Odessa Addison, Robin L. Marcus, Paul C. LaStayo, Alice S. Ryan, *Intermuscular Fat: A Review of the Consequences and Causes*, International Journal of Endocrinology, vol. 2014, Article ID 309570, 11 pages, 2014. https://doi.org/10.1155/2014/309570

[16] https://www.sciencedirect.com/topics/agricultural-and-biological-sciences/adipose-tissue (accessed on 01.03.22)

[17] Lehr S, Hartwig S, Sell H., *Adipokines: a treasure trove for the discovery of biomarkers for metabolic disorders.* Proteomics Clin Appl. 2012 Jan;6(1-2):91-101. doi: 10.1002/prca.201100052. Epub 2011 Dec 27. PMID: 22213627.

[18] Kershaw EE, Flier JS*., Adipose tissue as an endocrine organ*. J Clin Endocrinol Metab. 2004 Jun;89(6):2548-56. doi: 10.1210/jc.2004-0395. PMID: 15181022.

[19] Bouchard C., *Genetics of Obesity: What We Have Learned Over Decades of Research.* Obesity (Silver Spring). 2021 May;29(5):802-820. doi: 10.1002/oby.23116. PMID: 33899337.

[20] Keith, S., Redden, D., Katzmarzyk, P. et al., *Putative contributors to the secular increase in obesity: exploring the roads less traveled.* Int J Obes 30, 1585–1594 (2006). https://doi.org/10.1038/sj.ijo.0803326

[21] Speakman, J. R., Stubbs, R. J., Mercer, J. G., *Does body mass play a role in the regulation of food intake?,* Proceedings of the nutrition society (2002), 61, 473-487, DOI: 10.1079/PNS2002194

[22] Müller MJ, Bosy-Westphal A, Heymsfield SB. *Is there evidence for a set point that regulates human body weight?*. *F1000 Med Rep*. 2010;2:59. Published 2010 Aug 9. doi:10.3410/M2-59

[23] Schwartz MW, Seeley RJ, Zeltser LM, et al., *Obesity Pathogenesis: An Endocrine Society Scientific Statement*. Endocr Rev. 2017;38(4):267-296. doi:10.1210/er.2017-00111

[24] Leibel RL, Rosenbaum M, Hirsch J., *Changes in energy expenditure resulting from altered body weight.* N Engl J Med. 1995 Mar 9;332(10):621-8. doi: 10.1056/NEJM199503093321001. Erratum in: N Engl J Med 1995 Aug 10;333(6):399. PMID: 7632212.

[25] Pasquet P, Apfelbaum M., *Recovery of initial body weight and composition after long-term massive overfeeding in men*. Am J Clin Nutr. 1994 Dec;60(6):861-3. doi: 10.1093/ajcn/60.6.861. PMID: 7985625.

[26] Diaz EO, Prentice AM, Goldberg GR, Murgatroyd PR, Coward WA., *Metabolic response to experimental overfeeding in lean and overweight healthy volunteers.* Am J Clin Nutr. 1992 Oct;56(4):641-55. doi: 10.1093/ajcn/56.4.641. PMID: 1414963.

[27] Rexford S. Ahima and Jeffrey S. Flier, *Leptin,* Annual Review of Physiology 2000 62:1, 413-437

[28] Martin G. Myers, Michael A. Cowley, Heike Münzberg*, Mechanisms of Leptin Action and Leptin Resistance,* Annual Review of Physiology 2008 70:1, 537-556

[29] Myers MG Jr, Heymsfield SB, Haft C, et al. *Challenges and opportunities of defining clinical leptin resistance.* Cell Metab. 2012;15(2):150-156. doi:10.1016/j.cmet.2012.01.002

[30] Wang H, Eckel RH., *Lipoprotein lipase: from gene to obesity.* Am J Physiol Endocrinol Metab. 2009 Aug;297(2):E271-88. doi: 10.1152/ajpendo.90920.2008. Epub 2009 Mar 24. PMID: 19318514.

[31] Hall KD, Chen KY, Guo J, Lam YY, Leibel RL, Mayer LE, Reitman ML, Rosenbaum M, Smith SR, Walsh BT, Ravussin E., *Energy expenditure and body composition changes after an isocaloric ketogenic diet in overweight and obese men.* Am J Clin Nutr. 2016 Aug;104(2):324-33. doi: 10.3945/ajcn.116.133561. Epub 2016 Jul 6. PMID: 27385608; PMCID: PMC4962163.

[32] National Institutes of Health, National Heart, Lung, and Blood institute. *Managing Overweight and Obesity in Adults: A Systematic Evidence Review from the Obesity Expert Panel.* 2013. Available at: https://www.nhlbi.nih.gov/health-topics/managing-overweight-obesity-in-adults (accessed on 15.08.22)

[33] Li R, Xia J, Zhang XI, Gathirua-Mwangi WG, Guo J, Li Y, McKenzie S, Song Y. *Associations of Muscle Mass and Strength with All-Cause Mortality among US Older Adults.* Med Sci Sports Exerc. 2018 Mar;50(3):458-467. doi: 10.1249/MSS.0000000000001448. PMID: 28991040; PMCID: PMC5820209.

[34] Mehler PS, Brown C. *Anorexia nervosa - medical complications*. J Eat Disord. 2015 Mar 31;3:11. doi: 10.1186/s40337-015-0040-8. PMID: 25834735; PMCID: PMC4381361.

[35] Pi-Sunyer X. *The medical risks of obesity*. Postgrad Med. 2009;121(6):21-33. doi:10.3810/pgm.2009.11.2074

[36] Calle EE, Thun MJ, Petrelli JM, Rodriguez C, Heath CW Jr. *Body-mass index and mortality in a prospective cohort of U.S. adults*. N Engl J Med. 1999 Oct 7;341(15):1097-105. doi: 10.1056/NEJM199910073411501. PMID: 10511607.

[37] Adela Hruby, JoAnn E. Manson, Lu Qi, Vasanti S. Malik, Eric B. Rimm, Qi Sun, Walter C. Willett, and Frank B. Hu, 2016: *Determinants and Consequences of Obesity,* American Journal of Public Health 106, 1656_1662, https://doi.org/10.2105/AJPH.2016.303326

[38] Fontaine K.R., Redden D.T., Wang C., Westfall A.O., Allison D.B., *Years of life lost due to obesity*. JAMA. 2003 Jan 8;289(2):187-93. doi: 10.1001/jama.289.2.187. PMID: 12517229.

[39] Allison DB, Downey M, Atkinson RL, Billington CJ, Bray GA, Eckel RH, Finkelstein EA, Jensen MD, Tremblay A. *Obesity as a disease: a white paper on evidence and arguments commissioned by the Council of the Obesity Society*. Obesity (Silver Spring). 2008 Jun;16(6):1161-77. doi: 10.1038/oby.2008.231. Epub 2008 May 8. PMID: 18464753.

[40] Mraz, M., & Haluzik, M. (2014). *The role of adipose tissue immune cells in obesity and low-grade inflammation,* Journal of Endocrinology, 222(3), R113-

R127. Retrieved Feb 27, 2022, from https://joe.bioscientifica.com/view/journals/joe/222/3/R113.xml

[41] De Heredia, F., Gómez-Martínez, S., & Marcos, A. (2012). *Obesity, inflammation and the immune system.* Proceedings of the Nutrition Society, 71(2), 332-338. doi:10.1017/S0029665112000092

[42] Madala, M. C., Franklin, B. A., Chen, A. Y., Berman, A. D., Roe, M. T., Peterson, E. D., Ohman, E. M., Smith, S. C., Gibler, W. B., & McCullough, P. A. (2008). *Obesity and Age of First Non-ST-Segment Elevation Myocardial Infarction*. Journal of the American College of Cardiology, 52(12), 979-985. https://doi.org/10.1016/j.jacc.2008.04.067

[43] Fox CS, Pencina MJ, Wilson PW, Paynter NP, Vasan RS, D'Agostino RB Sr. *Lifetime risk of cardiovascular disease among individuals with and without diabetes stratified by obesity status in the Framingham heart study.* Diabetes Care. 2008 Aug;31(8):1582-4. doi: 10.2337/dc08-0025. Epub 2008 May 5. PMID: 18458146; PMCID: PMC2494632.

[44] Wannamethee S.G., Shaper A.G., Walker M., *Overweight and obesity and weight change in middle aged men: Impact on cardiovascular disease and diabetes.* J Epidemiol Community Health. 2005 Feb;59(2):134-9. doi: 10.1136/jech.2003.015651. PMID: 15650145; PMCID: PMC1733005.

[45] Burke GL, Bertoni AG, Shea S, et al. *The impact of obesity on cardiovascular disease risk factors and subclinical vascular disease: the Multi-Ethnic Study of Atherosclerosis.* Arch Intern Med. 2008;168(9):928-935. doi:10.1001/archinte.168.9.928

[46] Wang TJ, Parise H, Levy D, D'Agostino RB Sr, Wolf PA, Vasan RS, Benjamin EJ. *Obesity and the risk of new-onset atrial fibrillation*. JAMA. 2004 Nov 24;292(20):2471-7. doi: 10.1001/jama.292.20.2471. PMID: 15562125.

[47] Drøyvold WB, Midthjell K, Nilsen TI, Holmen J. *Change in body mass index and its impact on blood pressure: a prospective population study.* Int J Obes (Lond). 2005 Jun;29(6):650-5. doi: 10.1038/sj.ijo.0802944. PMID: 15809666.

[48] Conen D, Ridker PM, Mora S, Buring JE, Glynn RJ. *Blood pressure and risk of developing type 2 diabetes mellitus: the Women's Health Study.* Eur Heart J. 2007 Dec;28(23):2937-43. doi: 10.1093/eurheartj/ehm400. Epub 2007 Oct 9. PMID: 17925342.

[49] Centers for Disease Control and Prevention (CDC). *Prevalence of overweight and obesity among adults with diagnosed diabetes--United States, 1988-1994 and 1999-2002.* MMWR Morb Mortal Wkly Rep. 2004 Nov 19;53(45):1066-8. PMID: 15549021.

[50] Look AHEAD Research Group, Pi-Sunyer X, Blackburn G, Brancati FL, Bray GA, Bright R, Clark JM, Curtis JM, Espeland MA, Foreyt JP, Graves K, Haffner SM, Harrison B, Hill JO, Horton ES, Jakicic J, Jeffery RW, Johnson KC, Kahn S, Kelley DE, Kitabchi AE, Knowler WC, Lewis CE, Maschak-Carey BJ, Montgomery B, Nathan DM, Patricio J, Peters A, Redmon JB, Reeves RS, Ryan DH, Safford M, Van Dorsten B, Wadden TA, Wagenknecht L, Wesche-Thobaben J, Wing RR, Yanovski SZ. *Reduction in weight and cardiovascular disease risk factors in individuals with type 2 diabetes: one-year results of the look AHEAD trial.* Diabetes Care. 2007 Jun;30(6):1374-83. doi: 10.2337/dc07-0048. Epub 2007 Mar 15. PMID: 17363746; PMCID: PMC2665929.

[51] Colditz GA, Willett WC, Rotnitzky A, Manson JE. *Weight gain as a risk factor for clinical diabetes mellitus in women.* Ann Intern Med. 1995 Apr 1;122(7):481-6. doi: 10.7326/0003-4819-122-7-199504010-00001. PMID: 7872581.

[52] Calle EE, Rodriguez C, Walker-Thurmond K, Thun MJ. *Overweight, obesity, and mortality from cancer in a prospectively studied cohort of U.S. adults*. N Engl J Med. 2003 Apr 24;348(17):1625-38. doi: 10.1056/NEJMoa021423. PMID: 12711737.

[53] Eliassen AH, Colditz GA, Rosner B, Willett WC, Hankinson SE. *Adult weight change and risk of postmenopausal breast cancer.* JAMA. 2006 Jul 12;296(2):193-201. doi: 10.1001/jama.296.2.193. PMID: 16835425.

[54] Thygesen LC, Grønbaek M, Johansen C, Fuchs CS, Willett WC, Giovannucci E. *Prospective weight change and colon cancer risk in male US health professionals.* Int J Cancer. 2008 Sep 1;123(5):1160-5. doi: 10.1002/ijc.23612. PMID: 18546286; PMCID: PMC3965300.

[55] Reijman M, Pols HA, Bergink AP, Hazes JM, Belo JN, Lievense AM, Bierma-Zeinstra SM. *Body mass index associated with onset and progression of osteoarthritis of the knee but not of the hip: the Rotterdam Study.* Ann Rheum

Dis. 2007 Feb;66(2):158-62. doi: 10.1136/ard.2006.053538. Epub 2006 Jul 12. PMID: 16837490; PMCID: PMC1798486.

[56] Riquelme A, Arrese M, Soza A, Morales A, Baudrand R, Pérez-Ayuso RM, González R, Alvarez M, Hernández V, García-Zattera MJ, Otarola F, Medina B, Rigotti A, Miquel JF, Marshall G, Nervi F. *Non-alcoholic fatty liver disease and its association with obesity, insulin resistance and increased serum levels of C-reactive protein in Hispanics.* Liver Int. 2009 Jan;29(1):82-8. doi: 10.1111/j.1478-3231.2008.01823.x. Epub 2008 Jul 16. PMID: 18647235.

[57] Adams LA, Angulo P. *Treatment of non-alcoholic fatty liver disease.* Postgrad Med J. 2006 May;82(967):315-22. doi: 10.1136/pgmj.2005.042200. PMID: 16679470; PMCID: PMC2563793.

[58] Petry NM, Barry D, Pietrzak RH, Wagner JA. *Overweight and obesity are associated with psychiatric disorders: results from the National Epidemiologic Survey on Alcohol and Related Conditions.* Psychosom Med. 2008 Apr;70(3):288-97. doi: 10.1097/PSY.0b013e3181651651. Epub 2008 Mar 31. PMID: 18378873.

[59] Mokdad AH, Ford ES, Bowman BA, Dietz WH, Vinicor F, Bales VS, Marks JS. *Prevalence of obesity, diabetes, and obesity-related health risk factors, 2001*. JAMA. 2003 Jan 1;289(1):76-9. doi: 10.1001/jama.289.1.76. PMID: 12503980.

[60] Kaess BM, Pedley A, Massaro JM, Murabito J, Hoffmann U, Fox CS. *The ratio of visceral to subcutaneous fat, a metric of body fat distribution, is a unique correlate of cardiometabolic risk.* Diabetologia. 2012;55(10):2622-2630. doi:10.1007/s00125-012-2639-5

[61] Ladeiras-Lopes R, Sampaio F, Bettencourt N, Fontes-Carvalho R, Ferreira N, Leite-Moreira A, Gama V. *The Ratio Between Visceral and Subcutaneous Abdominal Fat Assessed by Computed Tomography Is an Independent Predictor of Mortality and Cardiac Events.* Rev Esp Cardiol (Engl Ed). 2017 May;70(5):331-337. English, Spanish. doi: 10.1016/j.rec.2016.09.010. Epub 2016 Oct 17. PMID: 27765543.

[62] Frayn KN. *Visceral fat and insulin resistance - causative or correlative?* Br J Nutr. 2000 Mar;83 Suppl 1:S71-7. doi: 10.1017/s0007114500000982. PMID: 10889795.

[63] Björntorp P. *Abdominal fat distribution and disease: an overview of epidemiological data*. Ann Med. 1992 Feb;24(1):15-8. doi: 10.3109/07853899209164140. PMID: 1575956.

[64] Jensen MD. *Is visceral fat involved in the pathogenesis of the metabolic syndrome? Human model.* Obesity (Silver Spring). 2006 Feb;14 Suppl 1:20S-24S. doi: 10.1038/oby.2006.278. PMID: 16642959.

[65] Després JP. *Body fat distribution and risk of cardiovascular disease: an update*. Circulation. 2012 Sep 4;126(10):1301-13. doi: 10.1161/CIRCULATIONAHA.111.067264. PMID: 22949540.

[66] Bergman RN, Kim SP, Catalano KJ, Hsu IR, Chiu JD, Kabir M, Hucking K, Ader M. *Why visceral fat is bad: mechanisms of the metabolic syndrome.* Obesity (Silver Spring). 2006 Feb;14 Suppl 1:16S-19S. doi: 10.1038/oby.2006.277. PMID: 16642958.

[67] Després, JP., Lemieux, I. *Abdominal obesity and metabolic syndrome*. Nature 444, 881–887 (2006). https://doi.org/10.1038/nature05488

[68] Herold, G., u. Mitarbeiter, *Innere Medizin 2019*. 2019, Gerd Herold, Köln.

[69] Dympna Gallagher, Patrick Kuznia, Stanley Heshka, Jeanine Albu, Steven B Heymsfield, Bret Goodpaster, Marjolein Visser, Tamara B Harris, *Adipose tissue in muscle: a novel depot similar in size to visceral adipose tissue,* The American Journal of Clinical Nutrition, Volume 81, Issue 4, April 2005, Pages 903–910, https://doi.org/10.1093/ajcn/81.4.903

[70] Paul M. Coen, Bret H. Goodpaster, *Role of intramyocelluar lipids in human health,* Trends in Endocrinology & Metabolism, Volume 23, Issue 8, 2012, Pages 391-398, ISSN 1043-2760, https://doi.org/10.1016/j.tem.2012.05.009.

[71] Yim, JE., Heshka, S., Albu, J. et al. *Intermuscular adipose tissue rivals visceral adipose tissue in independent associations with cardiovascular risk.* Int J Obes 31, 1400–1405 (2007). https://doi.org/10.1038/sj.ijo.0803621

[72] Hassler EM, Deutschmann H, Almer G, Renner W, Mangge H, Herrmann M, et al. (2021) *Distribution of subcutaneous and intermuscular fatty tissue of the mid-thigh measured by MRI—A putative indicator of serum adiponectin level and individual factors of cardio-metabolic risk*. PLoS ONE 16(11): e0259952. doi:10.1371/journal.pone.0259952

[73] Balkau B, Deanfield JE, Després JP, Bassand JP, Fox KA, Smith SC Jr, Barter P, Tan CE, Van Gaal L, Wittchen HU, Massien C, Haffner SM.

International Day for the Evaluation of Abdominal Obesity (IDEA): a study of waist circumference, cardiovascular disease, and diabetes mellitus in 168,000 primary care patients in 63 countries. Circulation. 2007 Oct 23;116(17):1942-51. doi: 10.1161/CIRCULATIONAHA.106.676379. PMID: 17965405; PMCID: PMC2475527.

[74] WHO Expert Consultation. *Appropriate body-mass index for Asian populations and its implications for policy and intervention strategies*. Lancet. 2004 Jan 10;363(9403):157-63. doi: 10.1016/S0140-6736(03)15268-3. Erratum in: Lancet. 2004 Mar 13;363(9412):902. PMID: 14726171.

[75] Church TS, Kuk JL, Ross R, Priest EL, Biltoft E, Blair SN. *Association of cardiorespiratory fitness, body mass index, and waist circumference to nonalcoholic fatty liver disease.* Gastroenterology. 2006 Jun;130(7):2023-30. doi: 10.1053/j.gastro.2006.03.019. Erratum in: Gastroenterology. 2007 Jan;132(1):466. Biltoff, Emily [corrected to Biltoft, Emily]. PMID: 16762625.

[76] Machann J, Thamer C, Stefan N, Schwenzer NF, Kantartzis K, Häring HU, Claussen CD, Fritsche A, Schick F. *Follow-up whole-body assessment of adipose tissue compartments during a lifestyle intervention in a large cohort at increased risk for type 2 diabetes*. Radiology. 2010 Nov;257(2):353-63. doi: 10.1148/radiol.10092284. Epub 2010 Aug 16. PMID: 20713612.

[77] https://www.who.int/teams/noncommunicable-diseases/surveillance/systems-tools/steps (accessed on 15.08.22)

[78] Gill M Price, Ricardo Uauy, Elizabeth Breeze, Christopher J Bulpitt, Astrid E Fletcher. *Weight, shape, and mortality risk in older persons: elevated waist-hip ratio, not high body mass index, is associated with a greater risk of death,* The American Journal of Clinical Nutrition, Volume 84, Issue 2, August 2006, Pages 449–460, https://doi.org/10.1093/ajcn/84.2.449

[79] Patria Hume, Michael Marfell-Jones (2008), *The importance of accurate site location for skinfold measurement*, Journal of Sports Sciences, 26:12, 1333-1340, DOI: 10.1080/02640410802165707

[80] Borga M, West J, Bell JD, et al. *Advanced body composition assessment: from body mass index to body composition profiling.* Journal of investigative medicine 2018; 66, 1-9

[81] Inoue M, Bu N, Fukuda O, Okumura H. *Automated discrimination of tissue boundaries using ultrasound images of "ubiquitous echo".* Annu Int Conf

IEEE Eng Med Biol Soc. 2007;2007:1330-4. doi: 10.1109/IEMBS.2007.4352543. PMID: 18002209.

[82] Armellini F, Zamboni M, Robbi R, Todesco T, Rigo L, Bergamo-Andreis IA, Bosello O. *Total and intra-abdominal fat measurements by ultrasound and computerized tomography*. Int J Obes Relat Metab Disord. 1993 Apr;17(4):209-14. PMID: 8387970.

[83] Suzuki R, Watanabe S, Hirai Y, Akiyama K, Nishide T, Matsushima Y, Murayama H, Ohshima H, Shinomiya M, Shirai K, et al. *Abdominal wall fat index, estimated by ultrasonography, for assessment of the ratio of visceral fat to subcutaneous fat in the abdomen.* Am J Med. 1993 Sep;95(3):309-14. doi: 10.1016/0002-9343(93)90284-v. PMID: 8368228.

[84] Wagner DR. *Ultrasound as a tool to assess body fat.* J Obes. 2013;2013:280713. doi: 10.1155/2013/280713. Epub 2013 Aug 26. PMID: 24062944; PMCID: PMC3770049.

[85] Pineau JC, Filliard JR, Bocquet M. *Ultrasound techniques applied to body fat measurement in male and female athletes.* J Athl Train. 2009 Mar-Apr;44(2):142-7. doi: 10.4085/1062-6050-44.2.142. PMID: 19295958; PMCID: PMC2657029.

[86] Alberto Bazzocchi, Giacomo Filonzi, Federico Ponti, Ugo Albisinni, Giuseppe Guglielmi, Giuseppe Battista, *Ultrasound: Which role in body composition?,* European Journal of Radiology, Volume 85, Issue 8, 2016, Pages 1469-1480, ISSN 0720-048X, https://doi.org/10.1016/j.ejrad.2016.04.005.

[87] Müller W, Lohman TG, Stewart AD, Maughan RJ, Meyer NL, Sardinha LB, Kirihennedige N, Reguant-Closa A, Risoul-Salas V, Sundgot-Borgen J, Ahammer H, Anderhuber F, Fürhapter-Rieger A, Kainz P, Materna W, Pilsl U, Pirstinger W, Ackland TR. *Subcutaneous fat patterning in athletes: selection of appropriate sites and standardisation of a novel ultrasound measurement technique: ad hoc working group on body composition, health and performance, under the auspices of the IOC Medical Commission.* Br J Sports Med. 2016 Jan;50(1):45-54. doi: 10.1136/bjsports-2015-095641. PMID: 26702017; PMCID: PMC4717413.

[88] Müller W, Horn M, Fürhapter-Rieger A, Kainz P, Kröpfl JM, Maughan RJ, Ahammer H. *Body composition in sport: a comparison of a novel ultrasound imaging technique to measure subcutaneous fat tissue compared with*

skinfold measurement. Br J Sports Med. 2013 Nov;47(16):1028-35. doi: 10.1136/bjsports-2013-092232. Epub 2013 Sep 20. PMID: 24055780.

[89] Störchle P, Müller W, Sengeis M, Ahammer H, Fürhapter-Rieger A, Bachl N, Lackner S, Mörkl S, Holasek S. *Standardized Ultrasound Measurement of Subcutaneous Fat Patterning: High Reliability and Accuracy in Groups Ranging from Lean to Obese*. Ultrasound Med Biol. 2017 Feb;43(2):427-438. doi: 10.1016/j.ultrasmedbio.2016.09.014. Epub 2016 Nov 18. PMID: 27866704.

[90] Lackner S, Mörkl S, Müller W, Fürhapter-Rieger A, Oberascher A, Lehofer M, Bieberger C, Wonisch W, Amouzadeh-Ghadikolai O, Moser M, Mangge H, Zelzer S, Holasek SJ. *Novel approaches for the assessment of relative body weight and body fat in diagnosis and treatment of anorexia nervosa: A cross-sectional study.* Clin Nutr. 2019 Dec;38(6):2913-2921. doi: 10.1016/j.clnu.2018.12.031. Epub 2019 Jan 10. PMID: 30670293.

[91] Sengeis M, Müller W, Störchle P, Führhapter-Rieger A. *Body weight and subcutaneous fat patterning in elite judokas*. Scand J Med Sci Sports. 2019 Nov;29(11):1774-1788. doi: 10.1111/sms.13508. Epub 2019 Jul 17. PMID: 31265152; PMCID: PMC6851779.

[92] Kelso A, Trájer E, Machus K, Treff G, Müller W, Steinacker JM. *Assessment of subcutaneous adipose tissue using ultrasound in highly trained junior rowers.* Eur J Sport Sci. 2017 Jun;17(5):576-585. doi: 10.1080/17461391.2016.1277788. Epub 2017 Jan 25. PMID: 28120641.

[93] Störchle P. *Ultrasound Measurement of Subcutaneous Adipose Tissue Thickness: Methodical Improvements, Intra-Observer Reliability in Overweight and Obese Persons, and Fat Patterning Analyses.* Graz: Medical University of Graz; 2019.

[94] Sengeis M., *Anthropometry and subcutaneous adipose tissue patterning in elite athletes: Application of a novel ultrasound method*. Graz: Medical University of Graz; 2021.

[95] Kerr A., Hume P., *Non-imaging Method: Bioelectrical Impedance Analysis.* Best Practice Protocols for Physique Assessment in Sport, 2018/01/01, 101-116, DOI: 10.1007/978-981-10-5418-1_9

[96] Kramer H, Pickhardt PJ, Kliewer MA, Hernando D, Chen GH, Zagzebski JA, Reeder SB. *Accuracy of Liver Fat Quantification With Advanced CT, MRI,*

and Ultrasound Techniques: Prospective Comparison With MR Spectroscopy. AJR Am J Roentgenol. 2017 Jan;208(1):92-100. doi: 10.2214/AJR.16.16565. Epub 2016 Oct 11. PMID: 27726414; PMCID: PMC5204456.

[97] Yu L, Liu X, Leng S, Kofler JM, Ramirez-Giraldo JC, Qu M, Christner J, Fletcher JG, McCollough CH. *Radiation dose reduction in computed tomography: techniques and future perspective.* Imaging Med. 2009 Oct;1(1):65-84. doi: 10.2217/iim.09.5. PMID: 22308169; PMCID: PMC3271708.

[98] https://radiopaedia.org/articles/dual-energy-x-ray-absorptiometry-1 (accessed on 18.08.22)

[99] Garg MK, Kharb S. *Dual energy X-ray absorptiometry: Pitfalls in measurement and interpretation of bone mineral density*. Indian J Endocrinol Metab. 2013 Mar;17(2):203-10. doi: 10.4103/2230-8210.109659. PMID: 23776890; PMCID: PMC3683192.

[100] https://radiopaedia.org/articles/mri-2 (accessed on 18.08.22)

[101]https://en.wikipedia.org/wiki/Magnetic_resonance_imaging#Usage_by_organ_or_system (accessed on 18.08.22)

[102] https://radiopaedia.org/articles/dixon-method (accessed on 08.08.21)

[103] Guerini H, Omoumi P, Guichoux F, Vuillemin V, Morvan G, Zins M, Thevenin F, Drape JL. *Fat Suppression with Dixon Techniques in Musculoskeletal Magnetic Resonance Imaging: A Pictorial Review.* Semin Musculoskelet Radiol. 2015 Sep;19(4):335-47. doi: 10.1055/s-0035-1565913. Epub 2015 Nov 19. PMID: 26583362.

[104] Ma J. *Dixon techniques for water and fat imaging*. J Magn Reson Imaging. 2008 Sep;28(3):543-58. doi: 10.1002/jmri.21492. PMID: 18777528.

[105] Lins CF, Salmon CEG, Nogueira-Barbosa MH. *Applications of the Dixon technique in the evaluation of the musculoskeletal system*. Radiol Bras. 2021 Jan-Feb;54(1):33-42. doi: 10.1590/0100-3984.2019.0086. PMID: 33583975; PMCID: PMC7869722.

[106] https://mriquestions.com/best-method.html (accessed on 08.08.21)

[107] Mitsiopoulos N, Baumgartner RN, Heymsfield SB, Lyons W, Gallagher D, Ross R. *Cadaver validation of skeletal muscle measurement by magnetic*

resonance imaging and computerized tomography. J Appl Physiol (1985). 1998 Jul;85(1):115-22. doi: 10.1152/jappl.1998.85.1.115. PMID: 9655763.

[108] Fields DA, Teague AM, Short KR, Chernausek SD. *Evaluation of DXA vs. MRI for body composition measures in 1-month olds*. Pediatr Obes. 2015 Oct;10(5):e8-10. doi: 10.1111/ijpo.12021. Epub 2015 Mar 27. PMID: 25820269; PMCID: PMC4678888.

[109] Kamel E.G., McNeill G., van Wijk M.C.W., *Usefulness of Anthropometry and DXA in Predicting Intra-abdominal Fat in Obese Men and Women.* Obesity Research (2000), 8: 36-42. https://doi.org/10.1038/oby.2000.6

[110] Zaida R. C.-M., Warren P., Cesar R. L., Ricardo C. E., Solomon O. A., Wanda H. H., Timothy G. L., *Reproducibility of DXA in Obese Women*, Journal of Clinical Densitometry, Volume 5, Issue 1, 2002, Pages 35-44, ISSN 1094-6950, https://doi.org/10.1385/JCD:5:1:035.

[111] Gong W, Ren H, Tong H, Shen X, Luo J, Chen S, Lai J, Chen X, Chen H, Yu W. *A comparison of ultrasound and magnetic resonance imaging to assess visceral fat in the metabolic syndrome*. Asia Pac J Clin Nutr. 2007;16 Suppl 1:339-45. PMID: 17392130.

[112] Attanasio S, Forte SM, Restante G, Gabelloni M, Guglielmi G, Neri E. *Artificial intelligence, radiomics and other horizons in body composition assessment*. Quant Imaging Med Surg. 2020 Aug;10(8):1650-1660. doi: 10.21037/qims.2020.03.10. PMID: 32742958; PMCID: PMC7378090.

[113] Greco F, Mallio CA. *Artificial intelligence and abdominal adipose tissue analysis: a literature review.* Quant Imaging Med Surg. 2021 Oct;11(10):4461-4474. doi: 10.21037/qims-21-370. PMID: 34603998; PMCID: PMC8408793.

[114] Masoudi S, Anwar SM, Harmon SA, Choyke PL, Turkbey B, Bagci U. *Adipose Tissue Segmentation in Unlabeled Abdomen MRI using Cross Modality Domain Adaptation.* Annu Int Conf IEEE Eng Med Biol Soc. 2020 Jul;2020:1624-1628. doi: 10.1109/EMBC44109.2020.9176009. PMID: 33018306; PMCID: PMC8972795.

[115] Shen N, Li X, Zheng S, Zhang L, Fu Y, Liu X, Li M, Li J, Guo S, Zhang H. *Automated and accurate quantification of subcutaneous and visceral adipose tissue from magnetic resonance imaging based on machine learning.* Magn

Reson Imaging. 2019 Dec;64:28-36. doi: 10.1016/j.mri.2019.04.007. Epub 2019 Apr 18. PMID: 31004712.

[116] Zhou A, Murillo H, Peng Q. *Novel segmentation method for abdominal fat quantification by MRI*. J Magn Reson Imaging. 2011 Oct;34(4):852-60. doi: 10.1002/jmri.22673. Epub 2011 Jul 18. PMID: 21769972.

[117] Thörmer G, Bertram HH, Garnov N, Peter V, Schütz T, Shang E, Blüher M, Kahn T, Busse H. *Software for automated MRI-based quantification of abdominal fat and preliminary evaluation in morbidly obese patients.* J Magn Reson Imaging. 2013 May;37(5):1144-50. doi: 10.1002/jmri.23890. Epub 2012 Nov 2. PMID: 23124651.

[118] Guha Roy, Abhijit & Conjeti, Sailesh & Sheet, Debdoot & Katouzian, Amin & Navab, Nassir & Wachinger, Christian. (2017). *Error Corrective Boosting for Learning Fully Convolutional Networks with Limited Data*. 231-239. 10.1007/978-3-319-66179-7_27.

[119] Jegou, Simon & Drozdzal, Michal & Vázquez, David & Romero, Adriana & Bengio, Y.. (2017). *The One Hundred Layers Tiramisu: Fully Convolutional DenseNets for Semantic Segmentation*. 1175-1183. 10.1109/CVPRW.2017.156.

[120] Estrada S, Conjeti S, Ahmad M, Navab N, Reuter M. *Competition vs. concatenation in skip connections of fully convolutional networks.* International Workshop on Machine Learning in Medical Imaging 2018 Sep 16 (pp. 214-222). Springer, Cham.

[121] Estrada S, Lu R, Conjeti S, Orozco-Ruiz X, Panos-Willuhn J, Breteler MMB, Reuter M. *FatSegNet: A fully automated deep learning pipeline for adipose tissue segmentation on abdominal dixon MRI.* Magn Reson Med. 2020 Apr;83(4):1471-1483. doi: 10.1002/mrm.28022. Epub 2019 Oct 21. PMID: 31631409; PMCID: PMC6949410.

[122] Linder, N., Schaudinn, A., Garnov, N. et al. *Age and gender specific estimation of visceral adipose tissue amounts from radiological images in morbidly obese patients.* Sci Rep 6, 22261 (2016). https://doi.org/10.1038/srep22261

[123] Jimenez-Del-Toro O, Muller H, Krenn M, Gruenberg K, Taha AA, Winterstein M, Eggel I, Foncubierta-Rodriguez A, Goksel O, Jakab A, Kontokotsios G, Langs G, Menze BH, Salas Fernandez T, Schaer R, Walleyo A, Weber MA,

Dicente Cid Y, Gass T, Heinrich M, Jia F, Kahl F, Kechichian R, Mai D, Spanier AB, Vincent G, Wang C, Wyeth D, Hanbury A. *Cloud-Based Evaluation of Anatomical Structure Segmentation and Landmark Detection Algorithms: VISCERAL Anatomy Benchmarks.* IEEE Trans Med Imaging. 2016 Nov;35(11):2459-2475. doi: 10.1109/TMI.2016.2578680. Epub 2016 Jun 9. PMID: 27305669.

[124] Ronneberger O, Fischer P, Brox T. *U-net: Convolutional networks for biomedical image segmentation.* International Conference on Medical image computing and computer-assisted intervention 2015 Oct 5 (pp. 234-241). Springer, Cham.

[125] Liao, Zhibin & Carneiro, Gustavo. (2017). *A Deep Convolutional Neural Network Module that Promotes Competition of Multiple-size Filters*. Pattern Recognition. 71. 10.1016/j.patcog.2017.05.024.

[126] Bradski, G. (2000) *The OpenCV Library*. Dr. Dobb's Journal of Software Tools, 120; 122-125.

[127] Giavarina D. *Understanding Bland Altman analysis*. Biochem Med (Zagreb). 2015;25(2):141-151. Published 2015 Jun 5. doi:10.11613/BM.2015.015

[128] Bonekamp S, Ghosh P, Crawford S, Solga SF, Horska A, Brancati FL, Diehl AM, Smith S, Clark JM. *Quantitative comparison and evaluation of software packages for assessment of abdominal adipose tissue distribution by magnetic resonance imaging.* Int J Obes (Lond). 2008 Jan;32(1):100-11. doi: 10.1038/sj.ijo.0803696. Epub 2007 Aug 14. PMID: 17700582; PMCID: PMC3096530.

[129] Kullberg J, Johansson L, Ahlström H, Courivaud F, Koken P, Eggers H, Börnert P. *Automated assessment of whole-body adipose tissue depots from continuously moving bed MRI: a feasibility study*. J Magn Reson Imaging. 2009 Jul;30(1):185-93. doi: 10.1002/jmri.21820. PMID: 19557740.

[130] Cremona A, Hayes K, O'Gorman CS, Laighin CN, Ismail KI, Donnelly AE, Hamilton J, Cotter A. *Inter and intra-reliability of ultrasonography for the measurement of abdominal subcutaneous & visceral adipose tissue thickness at 12 weeks gestation.* BMC Med Imaging. 2019 Dec 17;19(1):95. doi: 10.1186/s12880-019-0393-6. PMID: 31847832; PMCID: PMC6916062.

[131] Liu KH, Chan YL, Chan WB, Kong WL, Kong MO, Chan JC. *Sonographic measurement of mesenteric fat thickness is a good correlate with*

cardiovascular risk factors: comparison with subcutaneous and preperitoneal fat thickness, magnetic resonance imaging and anthropometric indexes. Int J Obes Relat Metab Disord. 2003 Oct;27(10):1267-73. doi: 10.1038/sj.ijo.0802398. PMID: 14513076.

[132] Mauad FM, Chagas-Neto FA, Benedeti ACGS, et al. *Reproducibility of abdominal fat assessment by ultrasound and computed tomography.* Radiol Bras. 2017;50(3):141-147. doi:10.1590/0100-3984.2016.0023

[133] Suzuki R, Watanabe S, Hirai Y, Akiyama K, Nishide T, Matsushima Y, Murayama H, Ohshima H, Shinomiya M, Shirai K, et al. *Abdominal wall fat index, estimated by ultrasonography, for assessment of the ratio of visceral fat to subcutaneous fat in the abdomen.* Am J Med. 1993 Sep;95(3):309-14. doi: 10.1016/0002-9343(93)90284-v. PMID: 8368228.

[134] Ono T, Taniguchi N, Osawa M, Onoguchi A, Kaneko S, Nakazawa Y, Kawano M, Itoh K. *The usefulness of mesenterium thickness as an index of visceral fat accumulation.* J Med Ultrason (2001). 2003 Sep;30(3):153-61. doi: 10.1007/BF02481220. PMID: 27278305.

[135] Bazzocchi A, Filonzi G, Ponti F, Sassi C, Salizzoni E, Battista G, Canini R. *Accuracy, reproducibility and repeatability of ultrasonography in the assessment of abdominal adiposity*. Acad Radiol. 2011 Sep;18(9):1133-43. doi: 10.1016/j.acra.2011.04.014. Epub 2011 Jul 2. PMID: 21724427.

[136] Gong W, Ren H, Tong H, Shen X, Luo J, Chen S, Lai J, Chen X, Chen H, Yu W. *A comparison of ultrasound and magnetic resonance imaging to assess visceral fat in the metabolic syndrome.* Asia Pac J Clin Nutr. 2007;16 Suppl 1:339-45. PMID: 17392130.

[137] Kammerlander AA, Lyass A, Mahoney TF, Massaro JM, Long MT, Vasan RS, Hoffmann U. *Sex Differences in the Associations of Visceral Adipose Tissue and Cardiometabolic and Cardiovascular Disease Risk: The Framingham Heart Study.* J Am Heart Assoc. 2021 Jun;10(11):e019968. doi: 10.1161/JAHA.120.019968. Epub 2021 May 15. PMID: 33998254; PMCID: PMC8483556.

[138] Karastergiou K, Smith SR, Greenberg AS, Fried SK. *Sex differences in human adipose tissues - the biology of pear shape.* Biol Sex Differ. 2012;3(1):13. Published 2012 May 31. doi:10.1186/2042-6410-3-13

[139] Wells JC. *Sexual dimorphism of body composition*. Best Pract Res Clin Endocrinol Metab. 2007 Sep;21(3):415-30. doi: 10.1016/j.beem.2007.04.007. PMID: 17875489.

[140] Nedungadi, Thekkethil & Clegg, Deborah. (2009). *Sexual Dimorphism in Body Fat Distribution and Risk for Cardiovascular Diseases*. Journal of cardiovascular translational research. 2. 321-7. 10.1007/s12265-009-9101-1.

[141] *Physical status: the use and interpretation of anthropometry. Report of a WHO expert committee.* World Health Organ Tech Rep Ser. 1995;854:1–452.

[142] Calle EE, Thun MJ, Petrelli JM, Rodriguez C, Heath CW Jr. *Body-mass index and mortality in a prospective cohort of U.S. adults.* N Engl J Med. 1999;341:1097–1105. DOI: 10.1056/NEJM1 99910 07341 1501.

[143] Miazgowski T, Kucharski R, Sołtysiak M, Taszarek A, Miazgowski B, Widecka K. *Visceral fat reference values derived from healthy European men and women aged 20-30 years using GE Healthcare dual-energy x-ray absorptiometry*. PLoS One. 2017;12(7):e0180614. Published 2017 Jul 6.doi:10.1371/journal.pone.0180614

[144] Hirsch KR, Blue MNM, Trexler ET, Smith-Ryan AE. *Visceral adipose tissue normative values in adults from the United States using GE Lunar iDXA*. Clin Physiol Funct Imaging. 2019 Nov;39(6):407-414. doi: 10.1111/cpf.12593. Epub 2019 Oct 1. PMID: 31449721.

[145] Schweitzer L., Geisler C., Pourhassan M., Braun W., Glüer C.-C., Bosy-Westphal A., Müller M.J., *What is the best reference site for a single MRI slice to assess whole-body skeletal muscle and adipose tissue volumes in healthy adults?,* The American Journal of Clinical Nutrition, Volume 102, Issue 1, July 2015, Pages 58–65, https://doi.org/10.3945/ajcn.115.111203

[146] https://en.wikipedia.org/wiki/Normal_distribution (accessed on 28.05.22)

[147] Positano V, Cusi K, Santarelli MF, Sironi A, Petz R, Defronzo R, Landini L, Gastaldelli A. *Automatic correction of intensity inhomogeneities improves unsupervised assessment of abdominal fat by MRI.* J Magn Reson Imaging. 2008 Aug;28(2):403-10. doi: 10.1002/jmri.21448. PMID: 18666138.